Chair of Process Technology and Industrial Environmental Protection

Master's Thesis

Partial-load behaviour of fluidized-bed methanation

Marlene Lasser, BSc

November 2021

EIDESSTATTLICHE ERKLÄRUNG

Ich erkläre an Eides statt, dass ich diese Arbeit selbständig verfasst, andere als die angegebenen Quellen und Hilfsmittel nicht benutzt, und mich auch sonst keiner unerlaubten Hilfsmittel bedient habe.

Ich erkläre, dass ich die Richtlinien des Senats der Montanuniversität Leoben zu "Gute wissenschaftliche Praxis" gelesen, verstanden und befolgt habe.

Weiters erkläre ich, dass die elektronische und gedruckte Version der eingereichten wissenschaftlichen Abschlussarbeit formal und inhaltlich identisch sind.

Datum 01.11.2021

Unterschrift Verfasser/in
Marlene Lasser

ACKNOWLEDGEMENTS

First of all, I would like to thank Univ.-Prof. Dipl.-Ing. Dr.-Ing **Markus Lehner**, head of the chair of process technology and environmental protection at Montanuniversität Leoben, with whose help I could conduct my thesis in Switzerland at PSI. He introduced me to Tilman Schildhauer and the research group at PSI and also made the bureaucracy and the overall handling of my thesis very uncomplicated.

Also a big thank you to Dr. **Tilman Schildhauer**, who accepted my request for a master's thesis at PSI. His helpfulness and support made me feel welcome from the beginning. His knowledge and expertise in the field of methanation was of great value and he helped me not to get lost in details but to see the big picture.

The biggest thank you goes to my direct supervisor **Andreas Gantenbein**. He made it possible for me to get to know and understand the research field of methanation as well as programming in MATLAB. His expertise and helpfulness, in case of any questions or complications, supported me very much in carrying out the simulations and writing this thesis. Without him, I would have been lost many times and this thesis would have probably taken me forever to complete.

Thank you to Dr. **Serge Biollaz**, head of the thermo-chemical processes group at PSI, for his efforts to make my stay here as trouble-free and comfortable as possible.

I would also like to thank all colleagues and staff of the thermo-chemical processes group at PSI for the warm welcome to the team and the support during my master's thesis. The operators **Julian Indlekofer**, **Martin Künstle** and **Tanja Wieseler** were responsible for a smooth run of the experiments and a great help with all questions I had about the experimental setup.

Last but not least, I want to express my profound gratitude to my parents **Sissi and Siegi Lasser** for providing me with unfailing support and encouragement throughout my years of study and the process of writing this thesis. This achievement would not have been possible without them. Thank you.

Abstract

Partial-load behaviour of fluidized-bed methanation

The growth of variable renewable energy sources requires new solutions for a secure and continuous energy supply. The keys are innovative energy storage systems, where Power-to-Gas (PtG) is one promising concept. To respond to the transient energy production, a flexible PtG process chain is necessary. This thesis investigates the feasibility and limits of partial-load behaviour in a fluidized-bed methanation reactor as part of an innovative process design for biogas upgrading plants. The vision is a year-round operation in different utilization stages. To imitate those stages, different scenarios (0 % methanation determining the maximum requirement for the membrane unit, 100 % methanation determining the maximum requirement for the reactor and various partial loads using the given dimensions) are simulated in a MATLAB-based toolbox for an industrial-scale 200 Nm³/h plant consisting of a membrane unit and a methanation reactor as the main parts. After validating the membrane model, the objective is to find the right process parameters (e.g. number of membrane modules and reactor pressure) to meet the grid injection requirements. Different membrane properties and gas velocities are tested, and the process management is varied in terms of the number of compressors in use. In addition, proof-of-concept experiments are conducted to show the feasibility of full and partial load in a fluidized-bed methanation reactor.

Taking a well-established biogas upgrading plant as reference, the membrane model could successfully be validated. The determined number of membrane modules from the 0 % methanation scenario is sufficient for the full- and partial-load PtG scenarios to also meet the grid injection requirements. With the given reactor parameters from the full PtG scenarios, the minimum partial load was determined at 20 and 30 % respectively, depending on the membrane material and the number of compressors. If the chosen process parameters were not sufficient for the simulation and the grid requirements, a reduction in the number of membrane modules and/or the reactor pressure provided remedy. Using a higher system pressure, the full PtG scenario with one compressor requires the same number of membrane modules as the 0 % methanation scenario. For the experiments with a recycle stream, the minimum partial load was at 40 % while still meeting the grid injection requirements.

Kurzfassung

Teillastverhalten der Wirbelschichtmethanisierung

Der Anstieg der variablen erneuerbaren Energiequellen erfordert neue Lösungen für eine sichere und kontinuierliche Energieversorgung. Der Schlüssel dazu sind innovative Energiespeichersysteme, wobei Power-to-Gas (PtG) ein vielversprechendes Konzept darstellt. Um auf die ungleichmäßige Energieerzeugung reagieren zu können, ist eine flexible PtG-Prozesskette notwendig. In dieser Arbeit werden die Machbarkeit und die Grenzen des Teillastverhaltens in einem Wirbelschichtmethanisierungsreaktor als Teil eines innovativen Prozessdesigns für Biogasaufbereitungsanlagen untersucht. Die Vision ist ein ganzjähriger Betrieb in verschiedenen Auslastungsstufen. Um diese Stufen nachzubilden, werden in einer MATLAB-basierten Toolbox verschiedene Szenarien (0 % Methanisierung als Maximalanforderung an die Membraneinheit, 100 % Methanisierung als Maximalanforderung an den Reaktor und verschiedene Teillastfälle unter Verwendung der festgelegten Dimensionen) für eine 200 Nm³/h Industrieanlage, bestehend aus einer Membraneinheit und einem Methanisierungsreaktor als Hauptbestandteile, simuliert. Nach der Validierung des Membranmodells besteht das Ziel darin, die richtigen Prozessparameter (z.B.: Anzahl der Membranmodule und Reaktordruck) zu finden, um die Einspeisebedingungen zu erfüllen. Es werden verschiedene Membraneigenschaften und Gasgeschwindigkeiten getestet, und die Prozessführung wird hinsichtlich der Anzahl der verwendeten Kompressoren variiert. Darüber hinaus werden Proof-of-Concept Experimente durchgeführt, um die Machbarkeit von Voll- und Teillast in einem Wirbelschichtmethanisierungsreaktor zu zeigen.

Anhand einer gut etablierten Biogasaufbereitungsanlage konnte das Membranmodell erfolgreich validiert werden. Die ermittelte Anzahl an Membranmodulen aus dem 0 % Methanisierungsszenario ist für die Voll- und Teillast-PtG-Szenarien ausreichend, um auch dort die Anforderungen an die Netzeinspeisung zu erfüllen. Mit den gegebenen Reaktorparametern aus den Volllast-PtG-Szenarien wurde die minimale Teillast mit 20 bzw. 30 % ermittelt, abhängig vom Membranmaterial und der Anzahl der Kompressoren. Reichten die gewählten Prozessparameter für die Simulation und die Netzanforderungen nicht aus, schaffte eine Reduzierung der Membranmodulanzahl und/oder des Reaktordrucks Abhilfe. Mit einem höheren Systemdruck konnte das Volllast-PtG-Szenario mit nur einem Kompressor und der gleichen Anzahl an Membranmodulen betrieben werden wie das 0 % Methanisierungsszenario. Bei den Experimenten mit einem Kreislaufstrom lag die minimale Teillast bei 40 %, während die Bedingungen für die Netzeinspeisung noch erfüllt wurden.

Contents

1 Introduction

The increasing concern about the climate crisis and the exhaustibility and other challenges concerning non-renewable energy sources like crude oil, natural gas and coal caused an increase in variable renewable power production like solar and wind in many countries worldwide. One of the main challenges with variable power production is that their energy output does not overlap with the demand for energy consumption. For instance there are seasonal differences in hours of sunshine per day and of course a lack of sunshine at night time. To tackle this challenge, energy storage is a possible solution.

In terms of energy storage systems, the Power-to-Gas (PtG) concept is a promising choice for long-term storage of large amounts of energy. The PtG process chain consists of an electrolysis and an optional methanation step to convert electrical power into the energy-rich gases hydrogen (H_2) and/or methane (CH_4) which can then be distributed, stored and reutilized for power, heat, mobility or chemical applications. Even though the methanation step signifies additional efficiency losses, it has some major advantages. For instance, with 1,200 kWh/m^3, the volumetric energy storage density of methane is higher than that of any other storage system currently on the market, the existing infrastructure in form of the international natural gas grid simplifies the transport and storage of CH_4 immensely and it can be reutilized in numerous ways. Methanation technologies are known for a couple of decades now but were originally used to produce synthetic or substitute natural gas (SNG) from coal, crude oil and naphtha. With the aim to convert H_2 coming from volatile renewable energy sources to CH_4, the requirements changed significantly. Different reactor concepts were developed, each with its individual advantages and challenges. The common challenge in recent years is the flexibilization of the PtG concepts. To make the PtG process chain less sensitive to high electricity prices in winter, it is necessary to be able to respond to a transient power production in a fast and efficient manner (e.g. short start up and shut down times and a wide load range).

The aim of this work is to investigate one possible process concept for a biogas upgrading plant through simulation and proof-of-concept experiments. The biogas is either upgraded by means of CO_2 separation via a membrane unit or converted to methane, depending on seasonal and hourly availability of biogas and H_2. The focus and innovation of this thesis lies in the partial-load behaviour of a fluidized-bed methanation reactor. To design the whole process, the maximum capacities of the membrane unit and the methanation reactor, respectively, have to be taken into account. Therefore, the cases for 0 % methanation and 100 % methanation (full PtG) are investigated first. To look into a possible process and cost optimization, the full- and partial-load PtG scenarios are each simulated with one and two compressors respectively. The experiments are not performed in the simulated process design but are used to demonstrate the feasibility of partial-load methanation in a fluidized-bed methanation reactor. All scenarios (simulated and experiments) have the objective to meet the grid injection requirements for the national gas grid in Switzerland.

2 Problem definition

In the following, background information about the conventional energy system and its challenges is given to explain the motivation behind the research field of methanation and Power-to-Gas respectively. Also, the motivation for using biogas as the CO_2 source and the objectives of this thesis will be explained.

2.1 Motivation

In the late 1990s, the world's electric power sector was a highly centralized and integrated industry that was mostly state controlled. Since then, it transformed into a more efficient and lean business model, including private ownership. The main driver for the transformation and development of power system strategies and projects are increased concerns about global warming, the associated environmental regulations and the growing awareness of environmental issues. Other significant catalysts are the ongoing market restructuring processes and evolving regulations around the world, the increased volatility of oil prices, nuclear accidents like the one in Fukushima, Japan, which practically stalled future development of nuclear power in many countries, and the increased tensions in countries that are large exporters of oil and gas e.g., the Middle East, Latin America and Russia. All this resulted in new legislations providing support for the development of renewable energy sources in many countries worldwide. Especially wind and solar photovoltaic experienced a tremendous growth; from 2004 to 2014 the average annual growth in installed capacity increased by around 23 % and 51 % respectively and their combined contribution to the global electricity production was around 6.2 % in 2015. However, due to constantly changing wind conditions and sun irradiation rates, those two renewable energy sources have a high degree of variability, which leads to seasonal, weekly and daily fluctuations of the power supply. The electrical systems were not designed for this type of generation, and with an increasing share of variable renewable energy sources in the generation capacity and energy production, conventional plants need to adjust to the production variability. Other impacts of variable renewable energy sources on the electricity market are the requirement for expansion of transmission and distribution systems, unexpectedly emerging spare capacities at conventional plants and the need for increased flexibility of the generation assets. Affordable solutions to address these challenges can be divided into two categories: technologies and market redesign. Table 1 gives an overview of the included solutions. One of the solutions in the technology category is energy storage. [1]

Amongst the different energy storage technologies, e.g., pumped hydro, batteries, compressed air storage, Power-to-Gas (PtG) (which will be further explained in 3.1) represents an interesting choice for long-term storage of large amounts of energy. To avoid their curtailment, the surplus energy coming from renewable energy sources is used to produce H_2 via water or steam electrolysis. Since electrolysis is upstream to methanation, intermittent H_2 production, due to a fluctuating power supply, results in transient operation. In addition to the H_2 input stream, CO_2 can also fluctuate, e.g., with changes in the biogas production at a biogas plant.

These sudden changes in boundary conditions can be met with high capacity H_2- and/or CO_2-storage tanks to assure a constant inlet flow, which strongly increases the facility costs. To avoid the extra cost, it is inevitable that methanation reactors are operated dynamically. With a dynamic operation, the requirements for the catalyst and reactor change significantly. To overcome this challenge, two ways are known so far: the development of catalysts that can withstand severe temperature changes over a long operation time, or the adaption of methanation reactor concepts for dynamic operation. [2], [3]

Table 1: Solutions to decrease challenges by increased energy production variability [1]

Technologies	Market redesign
• improved forecasting	• capacity payments
• greater flexibility of generation	• emission trading scheme revision
• dynamic transfers	• faster scheduling of the electricity market
• transmission expansion	• negative market price
• distribution expansion/modification	• nodal pricing
• increased visibility of distributed generation	• larger balancing areas
• demand response	• pooling
• energy storage	• ancillary services

In terms of the CO_2 source for the methanation step, biogas is an interesting choice because it consists of methane ($\sim 60\ \%$), carbon dioxide ($\sim 40\ \%$) and some impurities. For the efficient use of biogas as vehicle fuel or for its injection into the natural gas grid, it has to be upgraded. There are several technologies available on the market to separate the carbon dioxide from the methane, namely amine scrubbers, water scrubbers, pressure swing adsorption (PSA) units, organic scrubbers and membrane units. The plus sides of membranes compared to the other technologies are among others, a lower energy consumption, no need for auxiliary materials and no emissions. Another major advantage is the ease of scalability, which is especially helpful when combining biogas upgrading, full PtG and partial-load PtG in one plant. [4]–[6]

2.2   Objectives

The aim of this work is to investigate dynamic-operation or partial-load behaviour in a fluidized-bed methanation reactor. To categorize the partial load, the two borderline cases 0 % methanation (e.g. biogas upgrading with a membrane unit in a biogas plant) and 100 % methanation (e.g. direct methanation of biogas via a full Power-to-Gas process concept) are examined first. The idea is to develop an industrial-scale process where it is possible to flexibly switch between all three operating modes. The goal of this thesis is the contribution of the 0 % methanation step and one out of three possible variants for the full PtG and partial-load PtG, respectively, to this development process.

Prior to the start of this thesis, a rate-based membrane model was developed at PSI, according to Makaruk and Harasek [7]. The validation of this model with experimental data from an existing and well-documented biogas plant is the first objective here. With the validated membrane model, a biogas upgrading plant of industrial scale (200 Nm³/h) will be simulated and the necessary number of membrane modules for the full- and partial-load PtG is determined. The next step is the simulation of the industrial-scale full PtG scenario, which determines the dimensions of the methanation reactor for the whole plant. To demonstrate the feasibility of this step, a set of experiments is conducted in a pilot plant (10 kW, TRL 5). Lastly, the partial-load PtG scenario is simulated, where CO_2 and H_2 are varied to the same extent, with the goal to identify the minimum partial load. The feasibility of this scenario will again be shown by experiments in the pilot-scale plant. The full- and partial-load PtG scenarios will be simulated including two compressors in the model, the main compressor at the beginning and a smaller one before the reactor. The last objective is to determine whether a cost reduction can be achieved by using only the main compressor. The goal for all scenarios is to achieve a product gas that can be fed into the existing gas grid. For the purpose of this thesis, an introduction to methanation will be provided in a literature study, followed by a comparison of different methanation technologies and an overview of different approaches to the flexibilization of methanation reactors as well as an overview of hollow-fibre membranes.

3   Theoretical Background

In this chapter, the theoretical background of this thesis is described. After a general introduction to methanation and the available technologies, an overview of flexibilization efforts and a description of hollow-fibre membranes is given. To end the project background, the simulation toolbox and pilot plant are presented, at which the experiments were conducted.

3.1   Methanation

Methanation describes the hydrogenation of carbon oxides (CO/CO_2) to methane (CH_4), which is a heterogeneously catalysed synthesis. The synthesis can be gas-catalytic or biological, the main differences lie in the type of catalyst and the carbon source. Table 2 gives an overview of the two methanation technologies, their range of operating conditions and the existing process concepts. A more detailed description follows in 3.2 and 3.3. [3], [8], [9]

Table 2: Overview of different methanation technologies for small scale plants [3], [8]

Gas-catalytic methanation (250 – 550 °C, 1 – 100 bar)	Biological methanation (20 – 70 °C, 1 – 10 bar)

two phases (gaseous reactants, solid catalyst):
 	
• fixed bed
   o adiabatic
   o cooled (polytropic)
• fluidized bed (close to isothermal)
• structured
   o honeycomb
   o microchannel (cooled)
   o sorption enhanced
	continuous stirred tank reactor (CSTR)

three phases (gaseous reactants, liquid heat carrier, solid catalyst) • 3 phase fluidized bed • bubble column (slurry)	others • membrane • trickle bed • fixed bed

After the discovery of the methanation reaction in 1902, methanation was mainly used for the removal of CO-traces from H_2-rich feed gases in ammonia plants. Later on, the aim shifted to producing synthetic or substitute natural gas (SNG) from coal, crude oil and naphtha, using the methanation reaction as the main synthesis process, which completely changed the requirements. Since the methanation reaction is strongly exothermic, the amount of reaction heat generated when converting gas with high CO concentrations to methane is significantly

higher than removing trace amounts of CO. The efficient heat dissipation was the main challenge in developing catalysed methanation reactor concepts. Nowadays, methanation is still widely used for gas purification purposes in chemical or petrochemical industries and to produce SNG from coal or biomass. In recent years, the methanation reaction finds a new application in the Power-to-Gas (PtG) concept, with new specific differences and challenges to overcome. [8], [10]

The idea behind PtG is that electrical power is converted into a gaseous chemical storage medium, namely the energy-rich gases hydrogen (H_2) and methane (CH_4). As many regions worldwide tend to expand the share of renewable energy sources in their energy system, they also have to deal with challenges that arise with a continuous increase of the volatile portion of power production. Particularly the power generation by wind energy or photovoltaic shows more temporal fluctuations than other renewables such as waterpower or biomass. To compensate for these fluctuations, energy storage systems, as well as high-capacity distribution systems, will play a crucial role in the intelligent integration of surplus supply from volatile production. Concerning the volumetric energy storage density, methane has by far the highest (1.200 kWh/m^3) of several storage systems currently on the market, due to its calorific value. Another major advantage is the existing infrastructure for the transport and storage of CH_4. For example, Germany's natural gas pipelines and underground storages could store a theoretical value of 400 TWh of energy in the form of methane in the near future. Further advantages are the numerous possibilities to reutilize methane. For instance, it can be used as fuel in the mobility sector or it can be reconverted to electricity. The main downsides of PtG are its rather low efficiency of 30 – 75 % (without reconverting to electricity: 50 – 75 %), due to the losses in each conversion step, and the high costs. The individual steps and their interrelation within the PtG system can be seen in Figure 1. [3], [8], [11]
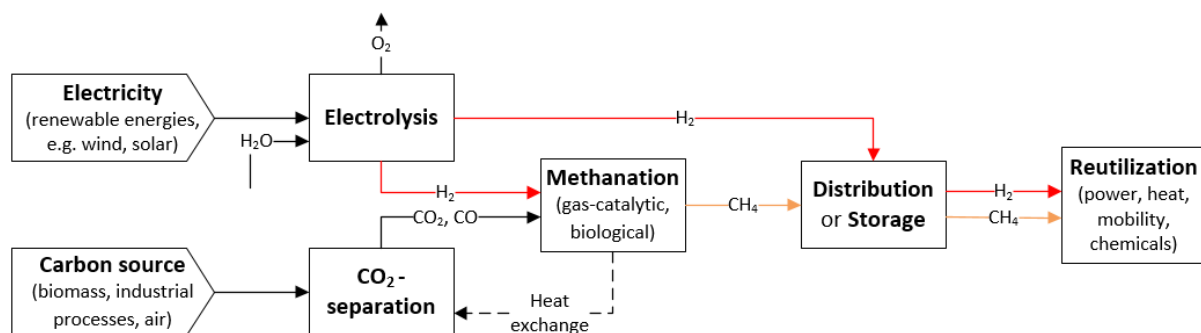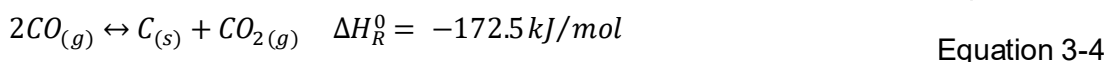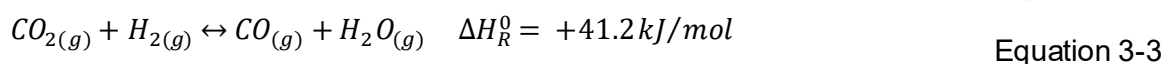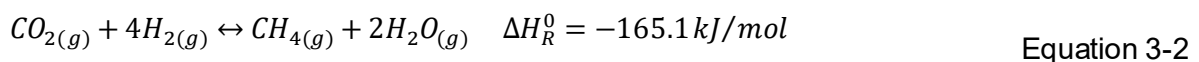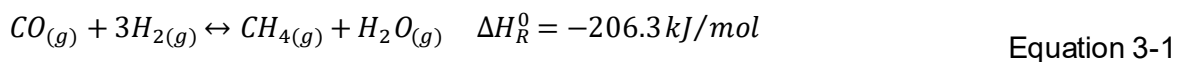

Figure 1: The Power-to-Gas process chain, schematic according to [3], [8]

3.2   Gas-catalytic methanation

Already in the earliest work about methanation, nickel was found to be a very efficient catalyst for gas catalytic methanation. It still is the material of choice, due to its low cost, relatively high activity and the fact that CO_2 methanation on nickel catalysts has a selectivity of almost 100 %. The main requirement to avoid deactivation of nickel-based catalysts is a high purity of the feed gas, especially halogeneous and sulphurous compounds contaminate the catalyst. Other active catalyst materials are ruthenium, rhodium, cobalt and iron. The requirements for a methanation reactor are still very high due to the following challenges. SNG produced from CO_2 methanation may have a lower calorific value than natural gas because of the lack of higher hydrocarbons. Götz et al. [3] state that to achieve a methane content higher than 90 %, a CO_2 conversion of almost 98 % is required. On the other hand, a high methane content is almost impossible to achieve with inert gases present or a hyper stoichiometric H_2/CO_2 ratio. For the large-scale production of SNG from coal, several reactor concepts were developed and have been erected and operated in China and the USA. However, due to smaller plant scales and differing feed gas compositions, the previously developed plant concepts for coal-to-gas plants are difficult or impossible to apply at small scale methanation plants. Novel concepts which are optimized for smaller plant sizes and intermittent or dynamic operation are required for the PtG chain. [3], [8], [9]

In terms of thermodynamics, four reactions play the biggest role in methanation processes, namely the hydrogenation of CO and CO_2, the reverse water gas shift reaction and the Boudouard reaction. The CO hydrogenation (Equation 3-1) was discovered in 1902 by P. Sabatier and J. B. Senderens and is also known as the Sabatier reaction. The water gas shift reaction (Equation 3-3) is important because instead of producing CH_4, it affects the H_2/CO ratio, which has far-reaching effects on the overall reaction products. Equation 3-2, the CO_2 hydrogenation, can be considered as a combination of Equation 3-1 and Equation 3-3. The Boudouard reaction (Equation 3-4) is an undesirable side reaction which can lead to a carbon deposition on the catalyst and has to be considered in gas-catalytic methanation. [3], [8], [9]

$$CO_{(g)} + 3H_{2(g)} \leftrightarrow CH_{4(g)} + H_2O_{(g)} \quad \Delta H_R^0 = -206.3 \, kJ/mol$$

Equation 3-1

$$CO_{2(g)} + 4H_{2(g)} \leftrightarrow CH_{4(g)} + 2H_2O_{(g)} \quad \Delta H_R^0 = -165.1 \, kJ/mol$$

Equation 3-2

$$CO_{2(g)} + H_{2(g)} \leftrightarrow CO_{(g)} + H_2O_{(g)} \quad \Delta H_R^0 = +41.2 \, kJ/mol$$

Equation 3-3

$$2CO_{(g)} \leftrightarrow C_{(s)} + CO_{2(g)} \quad \Delta H_R^0 = -172.5 \, kJ/mol$$

Equation 3-4

These strongly exothermic reactions require a good temperature regulation of the process to prevent thermodynamic limitation and catalyst sintering in the reactor. To meet this challenge, various reactor types were developed (see Table 2). The following reactor types were initially developed for steady-state operation, due to the need for dynamic operation (explained in 2.1), the research focus in recent years shifted. A summary of flexibilization efforts of different reactor types is given in 3.4. [3], [8]

3.2.1   Fixed-bed reactors

In a fixed-bed reactor, the catalyst, usually in pellet form and some millimetres in size, is dumped inside randomly, forming a preferably homogenous, static catalyst bed. For a good temperature regulation, the usual approach is an adiabatic reactor cascade, typically 2 – 5 reactors in series, with gas cooling, gas recycling and reaction heat recovery between each step. For cooled fixed-bed reactors, one reactor is sufficient. An example of an adiabatic fixed-bed methanation can be seen in Figure 2. One of the main benefits of the adiabatic fixed-bed type are the high reaction rate, the comparably low mechanical stress to the catalyst, a wide range of operation, a simple catalyst handling and a simple dimensioning and scale up, whilst the downsides are the high thermal load on the catalyst, that it has to withstand a wide temperature range (250 – 700 °C in adiabatic systems) to avoid cracking or sintering, further mass transfer limitations between the gases and the solid catalyst, the complex temperature control and the fact that multiple reactors in series and thus several compressors and/or heat exchangers are necessary. A cooled (isothermal) fixed-bed reactor contains cooling tube bundles or cooled plates, which simplifies the reactor setup, but the reactor itself is more expensive. [3], [8], [12]
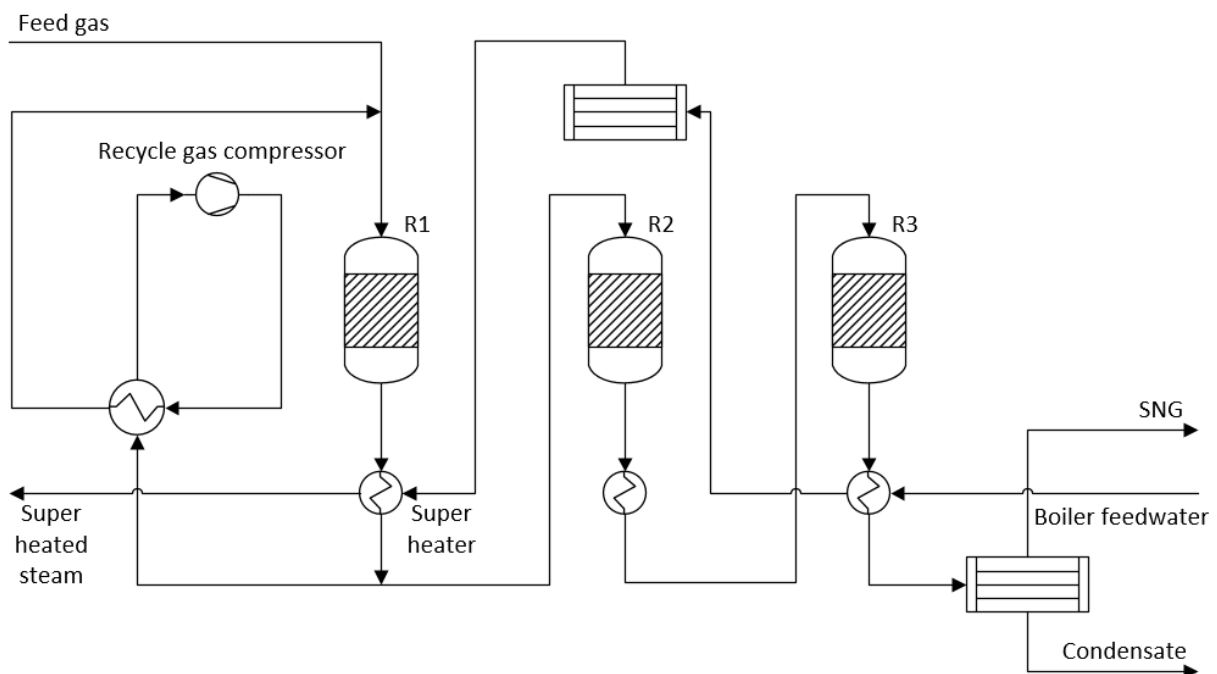

Figure 2: Example of an adiabatic fixed-bed methanation, adapted from [8], [10]

3.2.2   Fluidized-bed reactors

In a fluidized-bed reactor, the necessary force for the fluidization of the solid catalyst is applied by the gas. Due to the movement of particles, the temperature profile is approximately isothermal, which facilitates the control of the operation. An example of a fluidized-bed methanation can be seen in Figure 3. The main benefits of the fluidized-bed type are the more effective heat removal, small temperature gradients, a high specific surface area of the catalyst, and reduced mass transfer limitations, which allow for using one single reactor with a rather simplified design. The limited operating range due to superficial gas velocity, which cannot be too low to assure minimum fluidization conditions and cannot be too high to avoid catalyst carryover, can be extended with the reactor pressure as a further "screw". Other challenges which have to be handled are the high mechanical load due to the movement of the catalyst, resulting in abrasion of the particles and the wall of the reactor and leading to catalyst deactivation if inappropriate materials are chosen, and an incomplete CO_2 conversion caused by bubbling if the process is not properly controlled. [3], [8], [12]
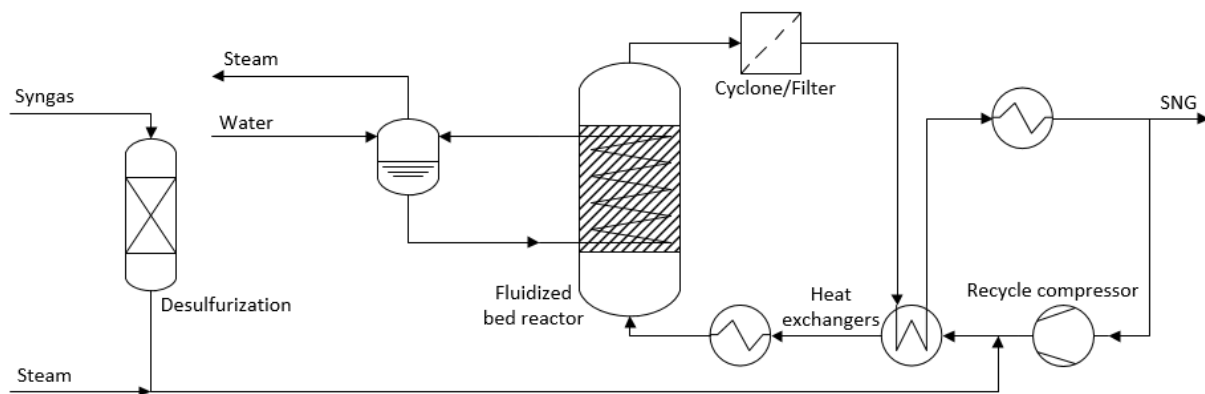

Figure 3: Example of a fluidized-bed methanation, adapted from [8], [10]

3.2.3   Structured reactors

In a structured microchannel reactor, an internal metallic structure is installed, which enhances the radial heat transport by two to three orders of magnitude, depending on the metallic material and compared to an adiabatic fixed-bed reactor, due to heat conduction through the metallic structure. An example of a structured microchannel methanation reactor can be seen in Figure 4. Another example of structured reactors are monolithic honeycombs, which consist of ceramic or metallic blocks with channels of different shapes (square, triangular, hexagonal). This reactor type was developed trying to solve the downsides of adiabatic fixed-bed reactors like temperature hot spots and high pressure drops. The main downside of the structured type is the costly production because of the complicated deposition of the catalyst on the structure and the fact that once the catalyst has been deactivated, the whole reactor has to be equipped with a new catalyst coating due to the difficulty of replacing the deactivated catalyst. [3], [13]
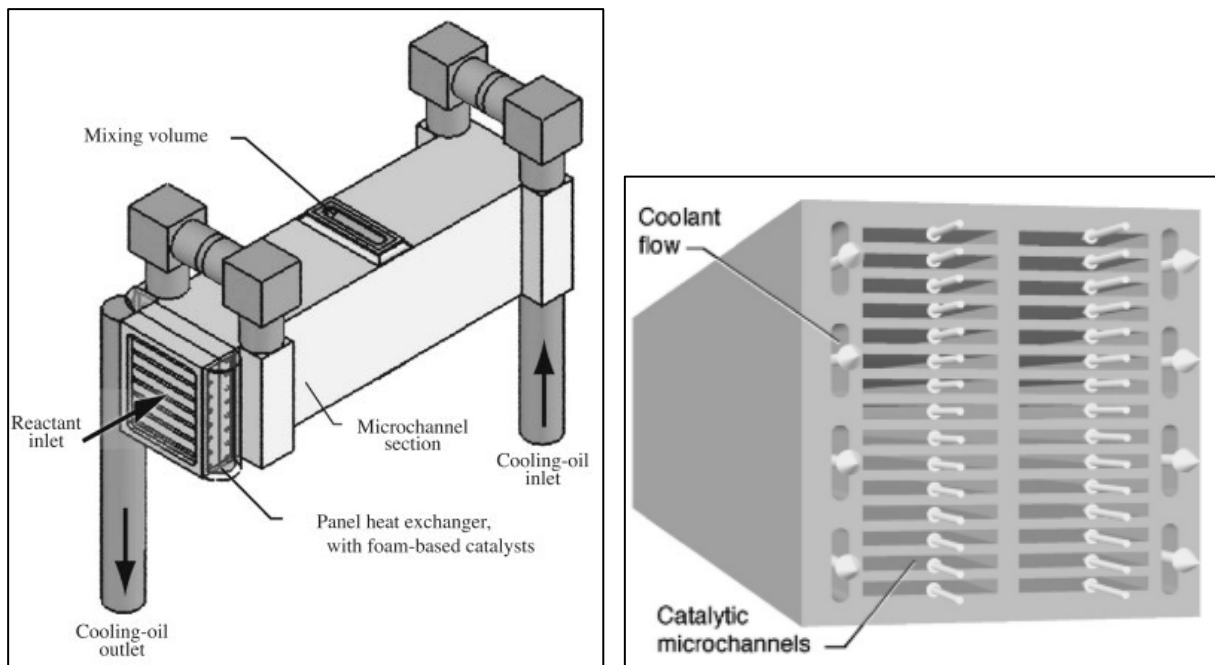
Figure 4: Example of a structured microchannel methanation reactor [14]

3.2.4   Three-phase reactors

In a three-phase reactor, fine catalyst particles are suspended in a liquid phase (e.g. a heat transfer oil like Dibenzyltoluene) as a result of the gas flow. The liquid phase has a high heat capacity, which promotes the heat release of the exothermic reactions and allows for effective and accurate temperature control, resulting in an almost isothermal temperature profile in the reactor. An example of a three-phase methanation can be seen in Figure 5. The main benefits of the three-phase type are the simple process design, the very effective heat removal, the isothermal conditions and the fact that it is less sensitive to fluctuating feed streams. Compared to the fluidized bed type, the catalyst abrasion is reduced and compared to the structured type the replacement of the catalyst is possible during operation. The challenges are a sophisticated hydraulic operation, gas-liquid mass transfer resistances, which may negatively influence the kinetics of the total process, the fact that backmixing is possible and the decomposition and evaporation of the heat transfer liquid. [3], [8], [12]
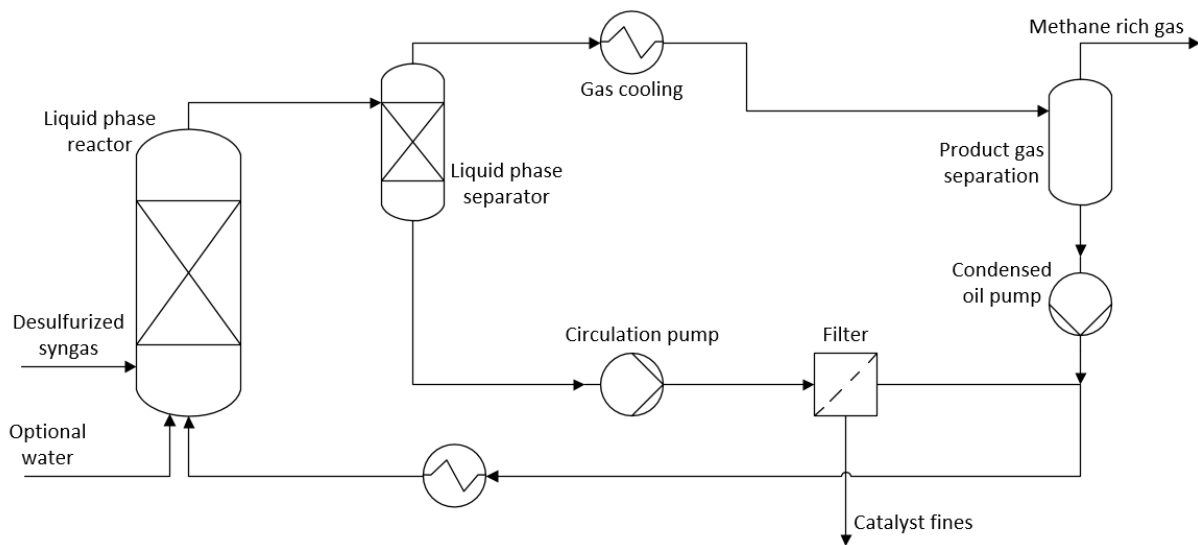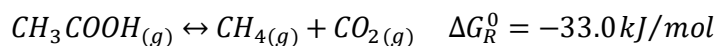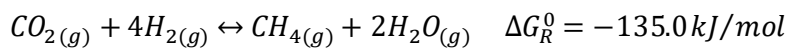
Figure 5: Example of a three-phase methanation, adapted from [8], [10]

3.3   Biological methanation

In the biological process route, methanogenic microorganisms (cell type: e.g. archaea) serve as biocatalysts. This methanation technology is particularly known in biogas processes, where the first process step is the hydrolysis of an organic substrate (biomass) to simple monomers (monosaccharide, amino acids, fatty acids), followed by the conversion of the monomers to acetate, carbon dioxide and hydrogen (acidogenesis, acetogenesis). For the methanation, two main reaction paths can be distinguished, the acetoclastic methanogenesis (depletion of acetate, Equation 3-5) and the hydrogenotrophic methanogenesis (CO_2 reduction with H_2, Equation 3-6). [3], [8]

$$CH_3COOH_{(g)} \leftrightarrow CH_{4(g)} + CO_{2(g)} \quad \Delta G_R^0 = -33.0\,kJ/mol$$

Equation 3-5

$$CO_{2(g)} + 4H_{2(g)} \leftrightarrow CH_{4(g)} + 2H_2O_{(g)} \quad \Delta G_R^0 = -135.0\,kJ/mol$$

Equation 3-6

The conditions during a biological methanation are anaerobic and the advantages compared to gas-catalytic methanation are the moderate operation temperatures of $20 - 70\,°C$ (mesophilic and thermophilic), which allow full conversion despite equilibrium limitations, the mostly ambient operation pressure and a higher tolerance against pollutant substances in the feed gases. The disadvantages compared to a two-phase gas-catalytic methanation reactor are the additional gas-liquid mass transfer resistance, since the biological methanation takes place within an aqueous solution, and the fact that nutrients like salts have to be provided for the microbes. The type of microorganism, cell concentration, reactor concept, pressure, pH-value and temperature are factors that influence the efficiency of bioreactors. An improvement of the gas-liquid mass transfer and thus the effective reaction rate is possible either by enhancing the mass transfer coefficient, e.g. through stirring, or by increasing the solubility, especially the poor solubility of H_2 in the broth (mainly water), e.g. through increasing the

pressure. A continuous stirred tank reactor (CSTR) is the most common reactor type for biological methanation, but also fixed-bed, trickle-bed and membrane reactors are being investigated. Compared to a CSTR, the methane formation rate in fixed-bed and trickle-bed reactors is significantly lower, but a stirrer is unnecessary, which results in a lower energy consumption. In general, two different process concepts are available for the biological path: integrative methanation and selective methanation. [3], [8]

3.3.1   Integrative biological methanation

The integrative biological methanation, also referred to as in-situ, utilizes an optimized biogas plant where, in addition to manure, sewage sludge or other biomass, H_2 is used as co-substrate. An exemplary process flow diagram for integrative biological methanation can be seen in Figure 6. While CO_2 is produced by the acetoclastic methanogenesis (Equation 3-5), part or all of it is in situ converted to CH_4 (Equation 3-6), resulting in a methane-rich biogas with a higher calorific value. The main benefits are the low investment costs as no further reactor is necessary, whilst the downsides are that only small methane formation rates are possible and that the process conditions cannot be adapted to optimal conditions (e.g. elevated temperature and pressure) for the hydrogenotrophic methanogenesis. [3], [8]
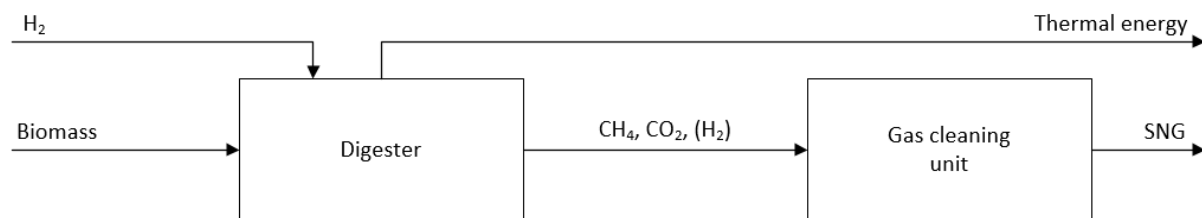

Figure 6: Exemplary process flow diagram for integrative biological methanation, adapted from [3]

3.3.2   Selective biological methanation

The selective biological methanation, also referred to as ex-situ, utilizes a separate bioreactor with adapted microbes under optimized process conditions. A self-sustaining operation is possible with an own carbon source, but the bioreactor can also be linked to a biogas process. An exemplary process flow diagram for selective biological methanation can be seen in Figure 7. In the bioreactor, methanogen cultures convert the pure gases into CH_4. The benefits are the possibility to increase the calorific value of biogas, the fact that biogas is not the only possible carbon source and that the process conditions and the reactor design can be adjusted with respect to the requirements of Equation 3-6. The main challenge and rate-limiting step, as with all biological reactor concepts, is the delivery of the gaseous H_2 to the microorganisms. [3], [8]
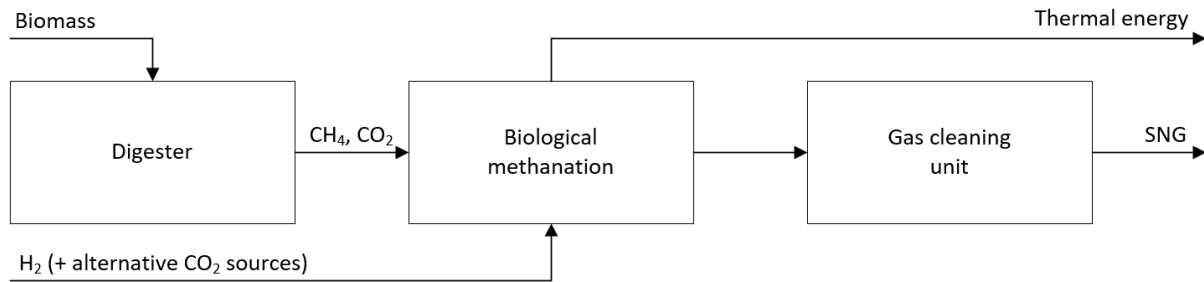
Figure 7: Exemplary process flow diagram for selective biological methanation, adapted from [3]

3.4   Flexibilization efforts for different methanation technologies

In the following, flexibilization efforts for some methanation technologies are presented. Namely for gas-catalytic fixed-bed and three-phase methanation as well as biological methanation. The main findings of the different efforts are summarized in Table 3.

Giglio et al. [2], present a one-dimensional dynamic model for a three-stage, multi-tubular, cooled fixed-bed reactor cascade. After designing the methanation unit for steady-state operation (number of tubes and length for each reactor), the transient response in terms of temperature profile and outlet methane content has been investigated for two cases: start up from hot standby condition and step reduction of the overall inlet flow. The findings were that the system requires about 130 s after a hot standby to reach the targeted methane content. At a reduction of the inlet flow to 80 %, an increase of the temperature peak was expected and verified, due to the longer residence time of the gaseous mixture in the tube. Since a further reduction of the inlet flow would imply a maximum temperature close to or even above the acceptability limit, a new process management with changed CO_2 staging strategy during partial-load operation is suggested. At lower partial loads, a fraction of the CO_2 bypasses the first and/or second reactor to decrease their maximum reached temperatures.

Matthischke et al. [15], investigated the unsteady-state operation in an adiabatic and cooled fixed-bed reactor respectively, with product recirculation using a one-dimensional model. To examine the load range, the volumetric flow rate at the system's inlet was varied corresponding to a superficial velocity at the reactor entrance. For the adiabatic fixed-bed reactor, the results show that with product recirculation, which cools the reactor, they can operate in a wide range of partial and excess load. The cooled reactor is less flexible because it is more sensitive to load changes of the volumetric flow rate, but the recycle of product gas allows a more stable operation under fluctuating feed conditions and the start-up time is considerably lower.

Lefebvre et al. [12], investigated the dynamic behaviour of a three-phase methanation reactor (a slurry bubble column reactor) using inlet gas velocity step changes to simulate load variation of a PtG facility. To do so, the reactor inlet gas velocity was shifted to a higher or lower level, while keeping the gas composition constant. To allow for the thermal stability of the system,

the suspension temperature and the outlet gas composition were monitored for at least 40 minutes before and after the gas velocity change. The results were obtained through experiments only, no simulations were performed. The reactor time constant т was evaluated for each transient experiment, to evaluate the reactor response to a gas velocity step change. The findings were that, while maintaining an isothermal temperature profile, the reactor showed rapid adaption to the load variations. The dead time, defined as the time interval between the gas velocity step change and the first change in outlet gas composition, is shorter for larger gas velocities. The reactor time constant т is only depending on the final gas velocity, which means that under the applied conditions, т is only a function of the gas residence time and that reactor hydrodynamics or reaction kinetics are not the limiting factors. Considering the use of slurry bubble column reactors for methanation purposes, this is a promising finding.

Inkeri et al. [16], developed a one-dimensional dynamic model for a continuously stirred biomethanation reactor with a novel approach that combines semi-fundamental modelling of gas-liquid mass transfer, hydrodynamics and biological reactions. With existing experimental data, the model was validated and used in a sensitivity analysis of critical parameters, a scale-up study of a biomethanation reactor and process dynamics studies. The trends observed in the varying experimental studies could be reproduced with the model. The findings were that biological parameters have minimal effect on methane production, that the model is very sensitive to the gas-liquid mass transfer properties (e.g. the geometry of the impeller and reactor) and that the required specific stirring power decreases as the size of the reactor increases. Considering the dynamics studies, it was shown that the modelled process is tolerant to large gradients in the input parameters and that the model can be used to perform scaled-up and dynamic studies of various reactor designs and different biomass solutions.

Table 3: Main findings of flexibilization efforts for different methanation technologies

	reactor type	simulation model type or experiments	investigated dynamics	investigated load range	results	reference
fixed-bed methanation	three-stage, multi-tubular, cooled fixed-bed reactor cascade	transient, one-dimensional, pseudo homogeneous mathematical model	start-up from hot standby and step reduction of the overall inlet flow	without CO_2 staging: 80 % with CO_2 staging: 70, 65, 60, 55, 50 and 45 %	130 s to reach the targeted CH_4 content after hot standby, 50 s to reach steady state at step reduction to 80 %, with CO_2 staging the minimum partial load is 45 %, CH_4 at reactor outlet is always above 95 %	[2]
	an adiabatic reactor (with partial product recycle) and a cooled fixed-bed reactor (without product recycle)	unsteady-state, one-dimensional, pseudo homogeneous fixed-bed recycle reactor model	load flexibility with emphasis on load range and start-up time	volumetric flow rate was varied corresponding to a superficial velocity adiabatic reactor: 0.19 – 1.94 m/s (10 – 100 %) cooled reactor: 0.6 – 1.5 m/s (40 – 100 %)	197 s for the cooled reactor to reach steady state after a warm start, 392 s for the adiabatic reactor; adiabatic reactor: maximum of methane content and temperature maximum are only slightly affected by the superficial velocity (broad load range); cooled reactor: narrower load range, very sensitive behaviour; recycle gas: 67 % H_2O and 33 % CH_4, after water separation a CH_4 content above 95 % should be possible	[15]

three-phase methanation	slurry bubble column reactor	no simulation, experiments	load variations using inlet gas velocity step changes	from 0.4 to 1.6 cm/s (25 – 100 %), 0.4 to 0.8 cm/s (25 – 50 %) and 0.8 to 1.6 cm/s (50 – 100 %), as well as the opposite step changes	the reactor time constant τ is halved when the gas velocity is doubled and reversely, τ is only a function of the gas residence time, reactor hydrodynamics or reaction kinetics are not the limiting factors influencing τ, the reactor temperature profile remained isothermal	[12]
biological methanation	continuously stirred biomethanation reactor	dynamic one-dimensional model for tall CSTRs	simple load changes, start-up and shut-down of the methanation	10 min full load – 10 min partial load (40 %) – 10 min full load – 10 min shut-down – 10 min partial load (80 %) – 10 min full load	steady state could be reached in less than 10 min for all load changes, the CH_4 content of the outflow gas does not remain above the desired 95 % level during load changes	[16]

3.5   Hollow-fibre membranes for gas separation

Hollow-fibre membrane modules are an efficient and energy-saving alternative for the gas separation step in biogas upgrading processes. Characteristically they are between 4 and 8 inches (10 – 20 cm) in diameter and 3 to 5 feet (1 – 1.6 m) long. The membrane is usually coated on the outside of a porous fibre support (see Figure 8, left), applied by a dip process where the polymer membrane is dissolved in a solvent. The filtration with hollow fibres is a flexible system, as the feed stream can either be on the inside of the fibre (as shown in Figure 8, left) or, more commonly, on the outside, so that the membrane is pressurized against the porous support. The individual fibres, normally several thousand per module, are bundled together at the ends (see Figure 8, right). During operation, the feed gas flows past the membrane at a high pressure. Consequently, a portion of the feed gas permeates through the membrane, enters the hollow-fibre channel and is removed as permeate on the low-pressure side of the membrane. The gas leaving the membrane on the high-pressure side is referred to as retentate. [6], [17]
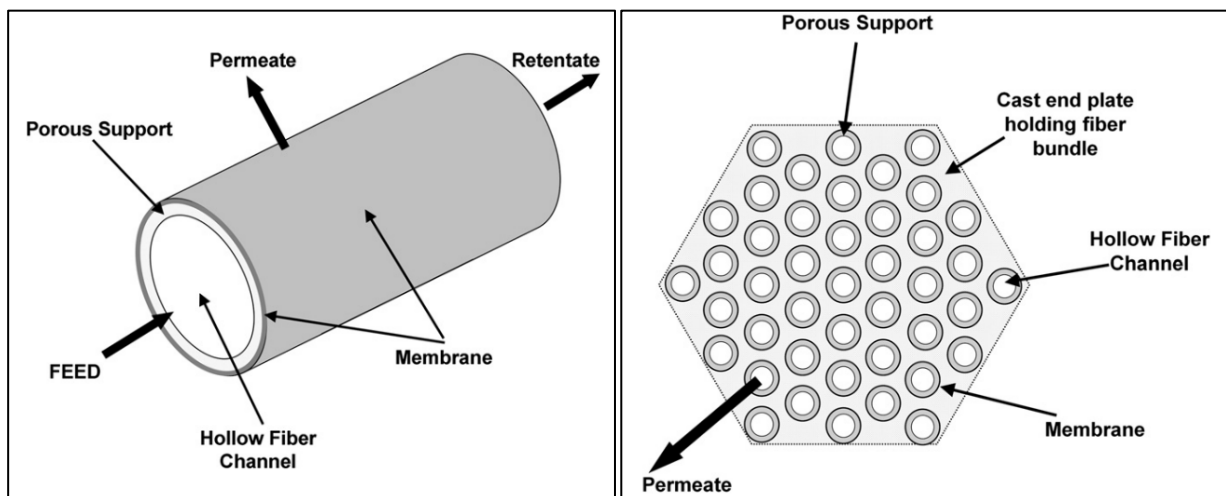

Figure 8: Schematic of a hollow fibre (left) and a hollow fibre bundle (right) used in gas separation [6]

The benefits of hollow-fibre membranes compared to other gas separation technologies are lower energy consumption, no requirement for auxiliary materials such as water or sorbents, no emissions into the environment, possible separation at ambient temperature, continuous separation process and high reliability, as there are no moving parts. The main drawbacks are chemical and thermal stability limits which have to be respected to avoid membrane fouling. Another feature that differentiates hollow-fibre membranes from other membrane types is the large membrane surface per module volume, which results in low space requirements, a simple modular setup and thus the possibility of flexible and easy expansion. [5], [6]

The principle of gas separation membranes is the selective permeation through a membrane surface, with the chemical structure determining the permeability of the selective layer. The driving force is the partial pressure difference between the gas on the retentate (high-pressure)

side and the gas on the permeate (low-pressure) side. A higher partial pressure difference results in a higher proportion of the gas permeating through the membrane. Permeability describes the rate at which a gas passes through a material and is usually measured in Barrer (Equation 3-7). The membranes' permeance is determined by dividing the permeability by the thickness of the selective layer and is expressed in terms of gas permeation units (gpu) (Equation 3-8). To increase the permeance of membranes made from a low-permeability material, the selective layer is made as thin as possible. [5], [17]

$$1 \, Barrer = \frac{10^{-10} \, cm^3 (STP) \, cm}{cm^2 \, s \, cmHg}$$

Equation 3-7

$$1 \, gpu = \frac{10^{-6} \, cm^3 (STP)}{cm^2 \, s \, cmHg}$$

Equation 3-8

3.6   Project background

The Thermochemical Processes (TCP) group at PSI has been working on the conversion of biogas from anaerobic digestion and the production of renewable CH_4 in PtG applications since 2015. In [18], the latest results as well as a concept idea for a flexible operation between biogas upgrading, full PtG and partial-load PtG are presented. The mentioned paper proposes a combination of three operating modes, biogas upgrading through CO_2 separation, and direct methanation of biogas, either full load or partial load, using renewable H_2. The idea is to switch between the three modes seasonally, e.g. biogas upgrading in winter, direct methanation with full PtG in summer and direct methanation with partial-load PtG in spring and autumn to react to price fluctuations on the electricity market. As all three processes require gas upgrading steps, the intention is to use the same type of membrane unit, which might cut down overall costs and lead to a higher yield of biogas. To further investigate this possibility, a rate-based membrane model, according to [7], and different variants for the direct methanation process were developed at PSI prior to this thesis. Variant 1 and variant 2 differ in the placement of the methanation reactor and are shown schematically in Figure 9. Regarding the membrane model, different permeability data sets, one from literature and one from experiments at PSI, are available, which were also researched prior to this thesis. The development and simulation of the biogas upgrading process as well as variant 2 for the direct methanation process (full- and partial-load PtG) will be investigated in this thesis.
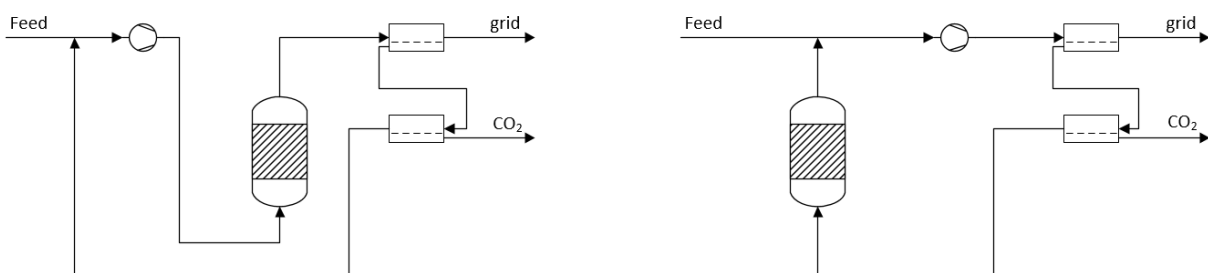

Figure 9: Schematic view of process variant 1 (left) and variant 2 (right)

3.7   Modelling

The modelling of the different scenarios took place in a MATLAB R2020b-based toolbox which was developed at PSI and interacts with Microsoft Excel and Athena Visual Studio. Within MATLAB, units and subunits interact with each other. The unit models are based on short-cut functions which are based on literature correlations. For a better understanding of the structure, Figure 10 shows the working principle of a modelling script. The units require subunits to function, which are used to calculate material properties. The input parameters (volume flow, CH_4 concentration, system pressure etc.) for the process simulations are read in from an Excel file, where it is easy to prepare the different scenarios in individual columns and test them one after the other with just one MATLAB command. The MATLAB script then runs through the units and subunits top down. The reactor unit accesses Athena where the reaction parameters, like reaction heat, gas concentrations at the reactor output etc., are determined and read back into MATLAB. For the reactor unit, two different models exist: the design model and the simulation model. With the design model, reactor dimensions as well as reaction parameters like the bubble size and reaction heat etc. can be determined. In the simulation model, the reaction parameters are determined with predefined reactor dimensions, which were e.g. obtained with the design model. The assumptions made for the differential equations applied in the BFB model are as follows:

- steady-state conditions
- isothermal conditions
- ideal gas behaviour
- no reaction in the bubble phase
- gas concentrations in the dense phase and on the catalyst particles are equal
- radial gas concentration differences are neglected
- deactivation mechanisms of the catalyst are neglected
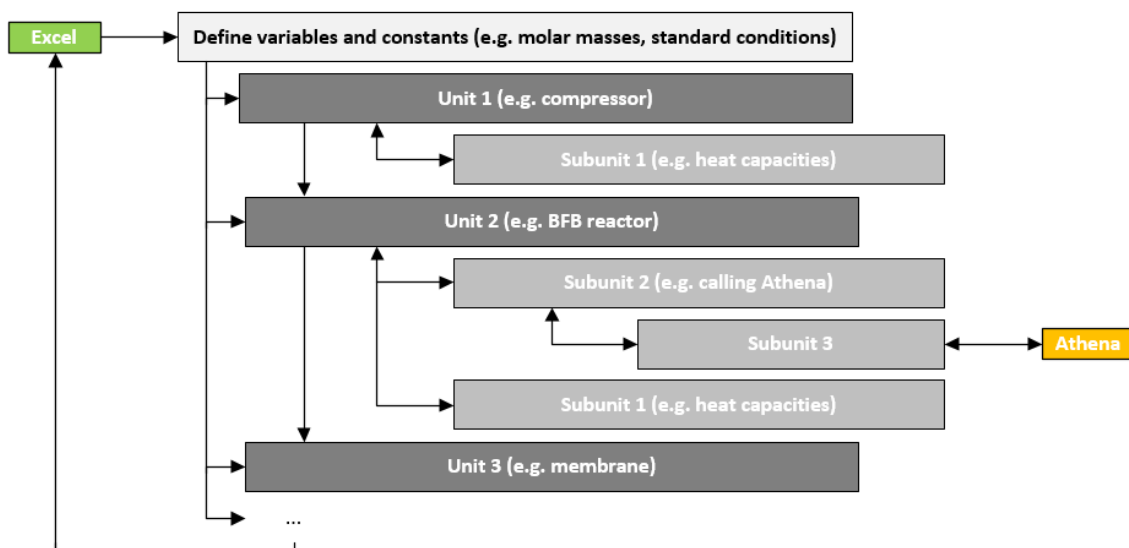

Figure 10: Working principle of the main modelling script in MATLAB

A detailed description of the pseudo-homogenous two-phase approach used for the modelling of this internally cooled fluidized-bed reactor can be found in [19] and especially in [20]. After finishing the calculations, the results are exported from MATLAB to Excel. At this point, it is noted that the units and subunits used in the simulation part of this thesis already existed and were put in the respective order to match the requirements of each scenario simulated. [19], [20]

The algorithm used in the membrane model was developed at PSI prior to this thesis according to [7] and was part of the existing MATLAB-based toolbox. It allows the calculation of multicomponent gas separation in hollow-fibre membrane modules in different configurations (co-current, counter-current and cross-flow) and is based on the iterative finite-difference Gauß-Seidel method. Only the counter-current configuration was used in this thesis, its finite-difference discretization for a single component i and in a domain consisting of c discrete points is presented in Figure 11. During the solution procedure, which is depicted in Figure 12, the feed flow is calculated from left to right and the permeate flow from right to left. [7]
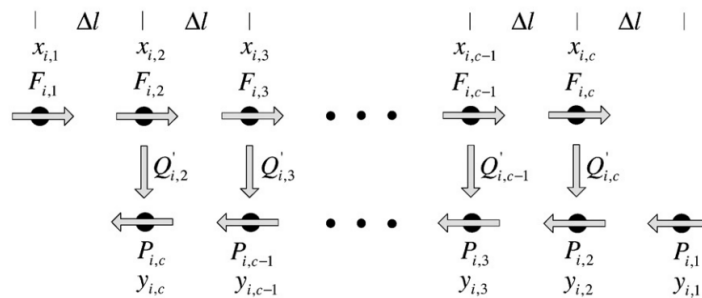
Figure 11: 1D finite-difference discretization for counter-current flow configuration [7]
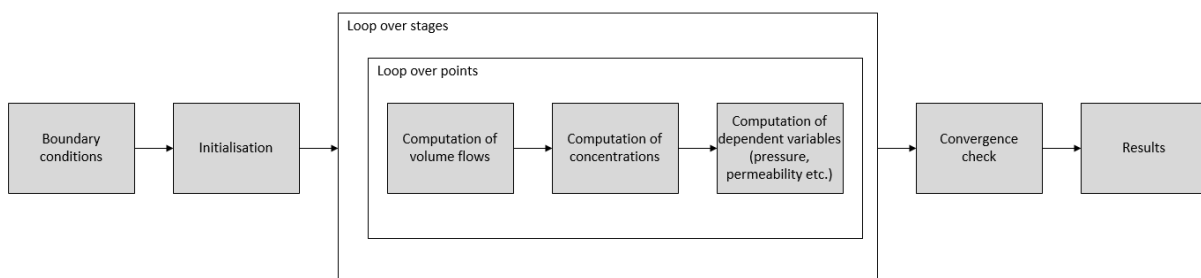
Figure 12: Solution procedure of the membrane model, adapted from [7]

Table 4 shows the input parameters for the membrane model. Changes in the membrane temperature (T_mem) are not considered by the model, because there is not sufficient experimental data available. The area of one membrane module (A_mod) as well as the length of one module (L_mod) refers to the Evonik membrane installed in COSYMA (see 3.8). The number of length units along the membrane (N_dL) and the relaxation factor (omega) are modelling parameters.

Table 4: Input parameters for the membrane model

T_mem	A_mod	L_mod	N_dL	omega
°C	m²	m	-	-
40	16.28	1	300 – 800	0.1 – 0.025

For the permeability data, a comparison between Matrimid® 5218 (permeability data according to [21], it is assumed that the Evonik membrane used in COSYMA is made of a similar material, case M) and experimental data (from previous experiments with the Evonik membrane used in COSYMA, case E) will be made for all process scenarios. The permeability data set for case M is summarized in Table 5. Case E consists of a function whose parameters were determined by fitting with experimental data. The function is not constant but describes the dependence of permeance on gas composition and different pressures (a publication regarding the membrane model and function is in preparation on the part of PSI).

Table 5: Permeability data set for case M, converted from [21]

H_2	CH_4	CO_2	H_2O*	N_2
mol m/(s m² Pa) *10^{-16}	mol m/(s m² Pa) *10^{-16}	mol m/(s m² Pa) *10^{-16}	mol m/(s m² Pa) *10^{-16}	mol m/(s m² Pa) *10^{-16}
58.56	0.703	24.39	58.56	0.736

*assumed to be identical with H_2

3.8   Experimental setup

A fully automated 10 – 20 kW scale reactor system named COSYMA (COntainer-based SYstem for MethAnation) was designed and built at the Paul Scherrer Institute (PSI), the heart of which is a bubbling fluidized-bed (BFB) reactor. The setup was designed to be used for CO_2 methanation, direct methanation of biogas or testing of membrane modules and a combination of the above. The diameter of the reactor is 5.2 cm, the catalyst mass at the beginning of this thesis' experiments was 800 g and the corresponding non-fluidized-bed height is 58 cm. A simplified flowsheet of the COSYMA setup is illustrated in Figure 13, with the measuring points identified. The pilot plant can either be operated by an arbitrary mixture of synthetic bottled gas (ports are available for CO_2, CO, C_2H_4, CH_4, H_2, N_2) or by real biogas from the digester of a biogas plant (for the experiments during this thesis, the COSYMA plant was installed at the SwissFarmerPower Inwil (SFPI)). Considering real biogas, the stream first is compressed to the desired system pressure, followed by a condenser cooled to 4 °C to remove liquid water and condensable contaminants. Next, the gas components CO, CO_2 and CH_4 are detected by a nondispersive infrared sensor (NDIR, SIEMENS Ultramat 23) and the mass flow is measured via a Coriolis flow meter (Endress+Hauser, Promass 500A), before the gas enters the gas cleaning unit. Harmful components, like organic sulphur, are removed there to protect the catalyst from deactivation. A detailed description of the gas cleaning unit can be found in [22].

The pilot plant is designed for a variety of scenarios. The gases from the bottled gas section (which are measured and controlled by mass-flow controllers (MFC, Bronkhorst EL-Flow)) can either be led through the gas cleaning unit or bypass it. The same applies to the methanation reactor and membrane unit, both of which can be bypassed if they are not required for an experiment. For methanation experiments, a small volume flow (approximately 100 Nml/min) of the gas mixture is continuously led to a micro gas chromatograph (mGC, VARIAN CP-4900) which is calibrated to measure H_2, CO_2, CH_4, N_2 and O_2 concentrations before the remaining gas stream is preheated to the reactor inlet temperature (approximately 340 °C) and mixed with steam. The added water is intended to prevent coking of the catalyst by shifting the equilibrium to the product side. The now humid gas stream enters the BFB reactor, where the methanation reaction takes place with a Ni/Al_2O_3 catalyst of Geldart particle type B. At this point, it is noted that the ratio of the entering gas velocity and the minimum velocity for fluidization at the reactor input has a lower limit to assure sufficient turbulence and an upper limit to prevent excessive carry-over of the catalyst. Inside the reactor, a lance is present to measure the temperature at different heights. After the reactor, catalyst particles that might be carried out, are removed from the reacted wet gas mixture in the particle filter unit. A condenser cooled to 4 °C then removes the water. The water entering the reactor in form of steam, as well as the water collected in the condenser after the reactor, is weighed to determine the produced water during the reaction. This gives information about the CO_2 conversion. The water removal after the reactor is also important to protect the membrane unit as it could get damaged by too much water entering. After the condenser, the gas is analysed again by an NDIR as well as a mGC before entering the membrane unit. At this point, the gas stream has an average composition of 88 % CH_4, 10.6 % H_2 and 1.4 % CO_2, according to [23]. The membrane unit aims to separate mainly the H_2 to reach the local gas grid injection specifications (> 96 % CH_4, < 4 % CO_2, < 2 % H_2 [24]). The permeate side of the membrane is equipped with a gas meter to determine the volumetric flow. As can be seen in Figure 13, the retentate and the permeate stream are merged and the whole output stream is measured by another gas meter. After this last measuring point, the produced bio methane is led back to the SFPI biogas plant. The used units Nl, Nml etc. refer to standard conditions at 1 atm and 0 °C. [18], [23]
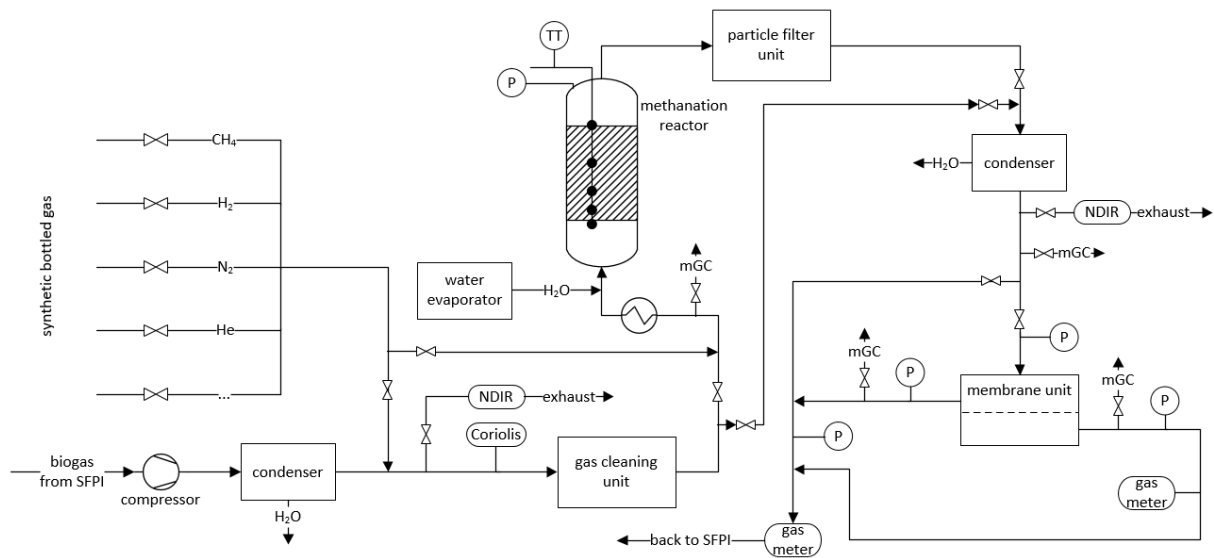
Figure 13: Simplified flowsheet of the COSYMA pilot plant

4   Methodology

This chapter describes the simulation procedure, the experiments and the analysis of the data for all four cases. The four cases correspond to a real biogas plant where experimental data is available to validate the membrane model, a simulated industrial-scale biogas upgrading plant (0 % methanation), a simulated industrial-scale full PtG plant (100 % methanation) and a simulated industrial-scale partial-load PtG plant with varying CO_2 and H_2 input. Also, the proof-of-concept experiments which were conducted with the COSYMA pilot plant are described.

4.1   Validation of the rate-based membrane model

To validate the present membrane model in the case of 0 % methanation, a comparison was made with an existing membrane upgrading plant, for which a detailed report exists. The comparison can be made because the modules used in this plant come from the same manufacturer as the one used in COSYMA, therefore it can be assumed that they are made of similar material and the assumptions made in the model are applicable. The summary of the report is as follows ([25] gives all the details about the existing plant). In the context of renovating the wastewater treatment plant in Reinach AG, CH, the wastewater association decided to start processing the sewage gas too and feed it into the natural gas grid. The construction and operation of a membrane unit for the upgrading of about 40 Nm^3/h raw biogas was realized. At the time, the membrane technology for biogas treatment was relatively new, and the project in Reinach AG had a demonstration character. The three-stage membrane process from Evonik Fibres GmbH was chosen for the processing of the raw biogas [26]. The membranes, 4 inches in diameter, consist of high-performance polymers and are characterized by different gas permeabilities in each separation step and a high carbon dioxide and methane selectivity. The project was successful, between 2015 and 2018 a total of 1.77 GWh or 166,099 Nm^3 of biogas was fed into the 5 bar natural gas grid. For the validation of the present membrane model, the process flow diagram from Reinach AG was reconstructed with the MATLAB toolbox (see 3.7) and is shown in Figure 14. The number of membrane modules in the different membrane stages (MEM 1, MEM 2 and MEM 3) were taken from the report. In MEM 1, one module is built in, and in MEM 2 and MEM 3 it is two modules each. Regarding the membrane area per module, an assumption of 97.68 m² was made. This corresponds to six times the area of the estimated membrane module in COSYMA. The assumption is based on the fact that the modules in Reinach AG have twice the diameter (factor four) and are of a newer type (factor 1.5, assumed). Also, the input parameters for two different operating points, which were the basis for the comparison, were taken from the report and are summarized in Table 6. The input parameters for the membrane model are listed in Table 4. As mentioned in 3.6, two different permeability data sets were used in the modelling process (case E and case M). The results (volume flows and CH_4 content in the grid and off-gas stream) from the simulation with the two different upgrading membrane types will be compared to the results from the plant in Reinach AG. [25]
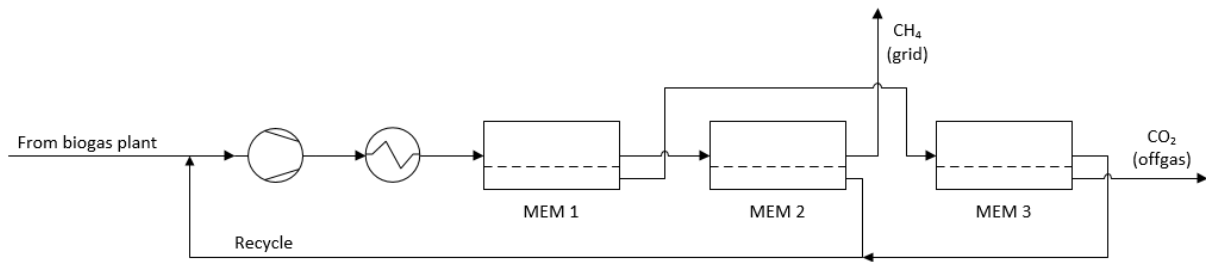
Figure 14: Process flow diagram for the simulation of the biogas plant in Reinach AG, following [25]

Table 6: Input parameters for the reconstructed biogas upgrading plant from [25]

	unit	operating point 1	operating point 2
system pressure	bara	17.5	17.8
biogas feed	Nm³/h	48.73	48.29
CH$_4$ in feed	Vol. %	62.8	
permeate pressure MEM 1	bara	2.2	
permeate pressure MEM 2	bara	1.05	
permeate pressure MEM 3	bara	1	

4.2   Reference case for 0 % methanation

The reference case for 0 % methanation is represented by a fictitious industrial-scale (200 Nm³/h) two-stage biogas upgrading plant scenario. This scenario determines the maximum requirement for the membrane unit. For the simulation, the MATLAB toolbox was set up according to Figure 15. The main input parameters can be found in Table 7. The input parameters for the membrane model can be found in Table 4. To optimize the number of membrane modules needed to achieve the grid injection requirements, an initial guess was made for both membrane stages. From there, the number was adjusted until the requirements were met. This was made for the two different upgrading membrane types. This scenario determines the necessary number of membrane modules or the necessary membrane area respectively for the full PtG and the partial-load PtG scenarios with two compressors. In contrast to the full- and partial-load PtG, the biogas upgrading scenario has two membrane stages instead of one. The number of membrane modules for MEM 1 from the biogas upgrading scenario can be applied to the full- and partial-load PtG scenarios with two compressors because the idea is to operate all three scenarios at the same plant. And with two compressors in place, the general conditions for MEM 1 are the same. In the case of just one compressor, the conditions change due to the higher permeate pressure and are not relatable to the biogas upgrading scenario.
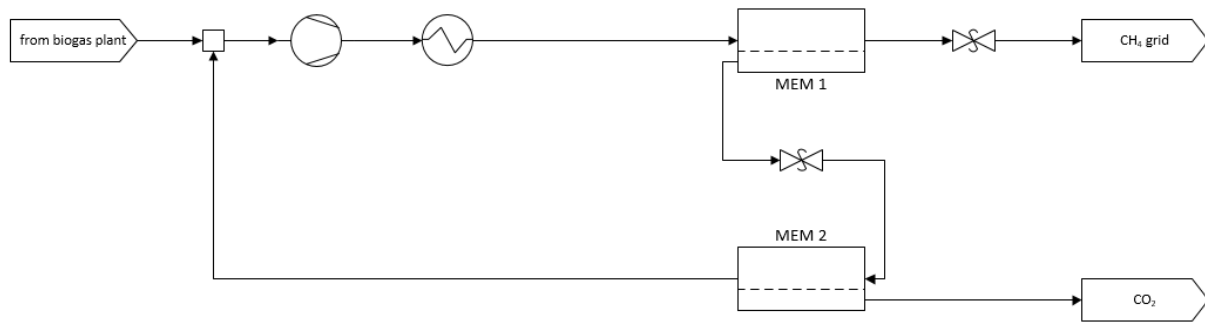
Figure 15: Process flow diagram for the simulation of an industrial-scale biogas upgrading plant

Table 7: Main input parameters for the simulation of an industrial-scale plant

case	feed	CH₄ in feed	system pressure	p_perm MEM 1	p_perm MEM 2	reactor pressure	permeability data cases
-	Nm³/h	Vol. %	bara	bara	bara	bara	-
bp[1]	200	60	15	3	1	-	E, M
f-PtG[2]	200	60	15	2	-	6	E, M
f-PtG-1[3]	200	60	15, 18, 20	4	-	4	E, M
pl-PtG[4]	40-150	60	15	2	-	6, 4, 2	E, M
pl-PtG-1[5]	40-150	60	15, 18, 20	4, 2	-	4, 2	E, M

[1] biogas plant, [2] full PtG with 2 compressors, [3] full PtG with 1 compressor, [4] partial-load PtG with 2 compressors, [5] partial-load PtG with 1 compressor

4.3   Reference case for 100 % methanation (full Power-to-Gas)

The reference case for 100 % methanation is represented by a fictitious industrial-scale (200 Nm³/h) full PtG scenario with the process management according to variant 2 (see Figure 9). Variant 2 is expected to be able to handle the partial load over a wide range because the reactor pressure can be set independently of the permeate pressure in the case with two compressors. This scenario determines the maximum requirement for the methanation reactor and thus the available reactor dimensions for the partial-load PtG scenario. It was carried out in four different ways: with either two compressors (according to Figure 16 (f-PtG)) or only the main compressor (f-PtG-1), and in each case with two different gas velocities (high and low), to determine if a cost reduction and technical feasibility can be achieved. For the simulation, the design model (see 3.7) was used and the MATLAB toolbox was set up according to Figure 16. The main input parameters were according to Table 4 and Table 7 with a reactor pressure of 6 bara and the number of membrane modules determined by the biogas upgrading plant setup (see Table 10) for the cases with two compressors. In contrast to the biogas upgrading scenario, the permeate pressure was set to 2 instead of 3 bara because only one membrane stage is present (the differential pressure of the second membrane is not relevant) and to maximize the efficiency. The remaining reactor input parameters can be found in Table 19 in the appendix. For the f-PtG-1 case, an optimization for the number of membrane modules had to be made again because the permeate pressure is significantly higher, which leads to a lower

differential pressure and a poorer separation performance in the membrane unit. All full PtG cases (different number of compressors, different gas velocities) were simulated with both upgrading membrane types (E and M). The results are the grid compliance at full PtG and four sets of reactor dimensions, which were then applied to the respective partial-load cases.
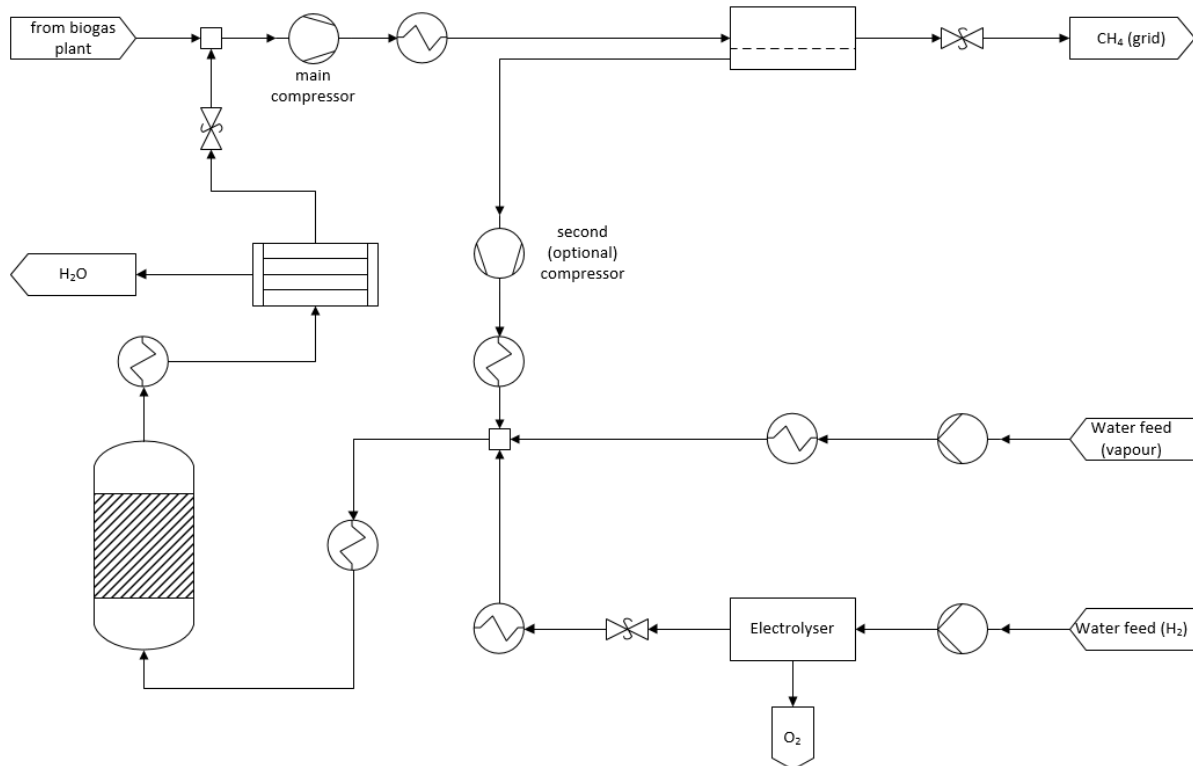

Figure 16: Process flow diagram for the simulation of the industrial-scale full- and partial-load PtG scenario

4.4   Full-load experiments with COSYMA

Full-load proof-of-concept experiments with a recycle of the permeate stream were performed with the COSYMA pilot plant. The setup is shown in Figure 17. The idea was to test the maximum operating limits of the compressor and the methanation reactor and to produce a product gas that meets the grid injection requirements with the help of the membrane unit. These experiments were the first time that COSYMA was operated with a recycle stream, so some test runs were conducted first to get a feeling for the handling. The start-up was performed without recycle and after COSYMA reached a steady-state condition, the recycle stream was connected at the inlet (see Figure 17). Since the permeate stream is recycled, the recycle is rich in H_2 and CH_4. The biogas and thus the CO_2 input is regulated by the compressor capacity, which can be varied between ~ 35 and 100 %. Because the recycle stream is connected in front of the compressor, it influences the biogas input. The test runs showed an H_2 accumulation in the system when no regulations were done manually. This is because of the H_2 surplus in the reactor input to ensure a high CO_2 conversion, which leads to around 10 % H_2 in the reactor output, then permeates through the membrane and is led back into the

system via the recycle stream. Over a short period of time, this leads to a bigger recycle stream and thus a smaller biogas stream, as the compressor is set to a certain capacity level. Without interference, the system will circulate H_2 over time and prevent CO_2 from entering. With a manual regulation, the idea is to keep the compressor at a steady capacity level and try to regulate the system with the H_2 input via the corresponding MFC. After a few runs, it was possible to operate the system close to steady state, with only minor adjustments in the H_2 input. To test the operating limits, the system pressure, compressor capacity and H_2 input were adjusted at the same time to prevent H_2 accumulation. The more or less steady-state set point with the highest H_2 input while complying with the grid requirements was declared as the maximum (full) load for the present system.
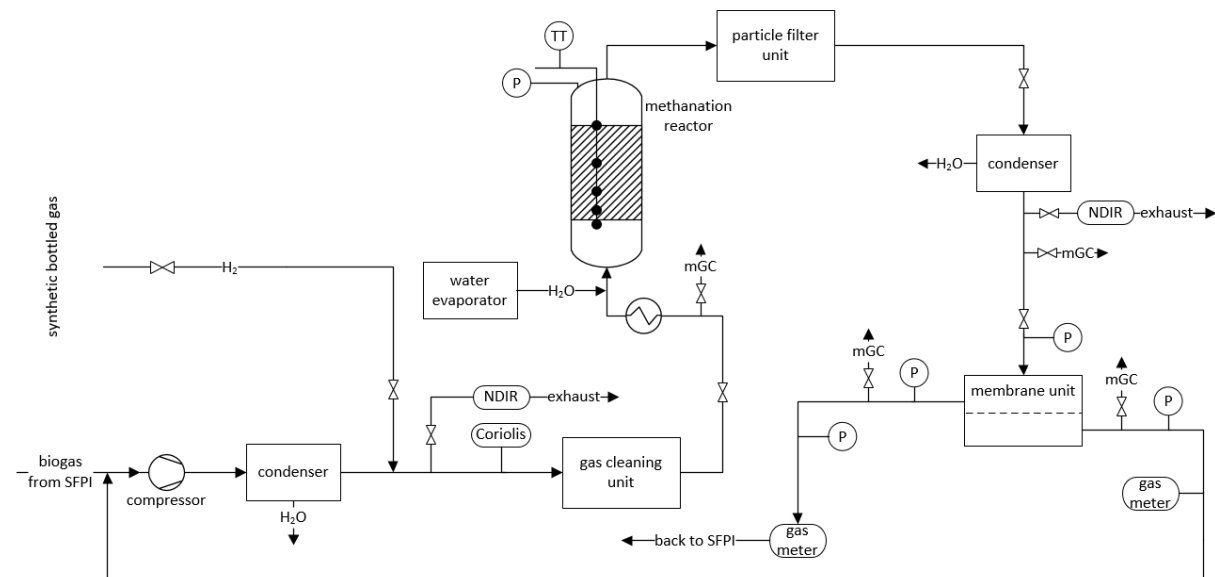

Figure 17: COSYMA setup for the full- and partial-load methanation experiments

The operating conditions of the full-load experiments are summarized in Table 8. In the experimental setup, the system pressure equals the methanation pressure (see Figure 17). Due to a CO_2 concentration above the grid injection requirements after the membrane, the compressor capacity, which regulates the biogas and thus the CO_2 input, was sometimes lower than 100 %, even though the system operated in full load. The maximum reactor pressure is 7 bara. As the compressor and membrane capacity were not always sufficient to meet the grid injection requirements, the system pressure was sometimes lower than that, even though the system operated in full load. The permeate pressure was set to 1 bara, due to the recycling of the permeate, it stabilized at 1.2 bara. These given conditions defined the H_2 addition.

Table 8: Operating conditions applied during full-load experiments

compressor capacity	H$_2$ addition	system pressure	permeate pressure
%	Nl/min	bara	bara
77 – 100	49.5 – 53	6.7 – 7	1.2

4.5   Partial-load Power-to-Gas

The partial-load PtG scenario represents the main subject of this thesis. Partial load can be achieved in different ways: CO_2 and H_2 can be varied at the same rate or at a different rate (e.g. one is constant, one is variable). In this thesis, the case where CO_2 and H_2 are varied at the same rate, so to say a change in capacity of the full PtG scenario, is investigated. In order for the CO_2 stream (biogas) to react to a transient H_2 supply, inflatable roofs in biogas plants can be used as a short term storage. For the simulation, the simulation model (see 3.7) with the respective reactor dimensions from the full PtG scenario (Table 11 and Table 13) was used and the MATLAB toolbox was set up according to Figure 16. The main input parameters were identical to the industrial-scale full PtG plant (see Table 4, Table 7 and Table 19) with a pressure in the reactor of 6 bara and the number of membrane modules determined by the biogas upgrading plant setup (see Table 10). For the pl-PtG-1 case, the optimized number of membrane modules from Table 12 was used, which results from the optimization done with the f-PtG-1 case (see 4.3). The goal was to find the minimum possible partial load where the membrane and reactor model still functions and the grid compliance can be met. To do so, the partial-load cases 75, 50, 40, 30 and 20 % were tested with the simulation toolbox, resulting in twenty different examples for cases with two compressors (five partial loads, two gas velocities and two permeability data cases) and sixty examples for the cases with one compressor (five partial loads, two gas velocities, two permeability data cases and three different system pressures). The results are the grid compliance for all partial-load PtG cases.

4.6   Partial-load experiments with COSYMA

Also, partial-load proof-of-concept experiments with a recycle of the permeate stream were performed with the COSYMA pilot plant, in the same setup as the full-load experiments (see Figure 17) and with the same strategy (see 4.4). The idea was to test different partial-load cases as well as the minimum operating limits of the compressor and the methanation reactor and to produce a product gas that meets the grid injection requirements with the help of the membrane unit. The operating conditions of the partial-load experiments are summarized in Table 9. The system pressure and thus the methanation pressure was varied because the compressor and the membrane capacity were not sufficient to meet the grid injection requirements at maximum pressure.

Table 9: Operating conditions applied during partial-load experiments

compressor capacity	H_2 addition	system pressure	permeate pressure
%	Nl/min	bara	bara
26 - 66	20 - 43	5.1 – 6.5	1.2

5   Results and discussion

In this chapter, the obtained results are summarized. For more clarity, the abbreviations f-PtG, f-PtG-1, pl-PtG and pl-PtG-1 are used. They stand for full Power-to-Gas with two compressors, full Power-to-Gas with one compressor, partial-load Power-to-Gas with two compressors and partial-load Power-to-Gas with one compressor respectively.

5.1   Validation of the rate-based membrane model

In Figure 18, the results for operating point 1 from the report from the biogas upgrading plant in Reinach AG are compared with the ones from the MATLAB simulation. The results for operating point 2 can be found in the appendix (Figure 25). For clarity reasons, only the results from operating point 1 are discussed here. Considering the output streams, the CH_4 rich grid stream and the CO_2 rich off-gas stream, the results from case E are very close to the ones from the report. For the grid volume flow and the off-gas volume flow, the deviation is 0.06 % and 1.06 % respectively. For the CH_4 concentration in the grid stream, the deviation is 0.08 %. The deviation for the CH_4 concentration in the off-gas stream is, with around 230 %, relatively high, but the simulated concentration is still lower than the 1 % limit. This limit does not refer to official regulations, it takes the methane loss from commercially operating, membrane-based biogas upgrading plants into account (see [27]) and is set to a low value, since the off-gas is released into the atmosphere. Considering case M (membrane properties of Matrimid, see [21]), the deviation for the grid volume flow, the off-gas volume flow, the CH_4 concentration in the grid and the CH_4 concentration in the off-gas are 5.99 %, 11 %, 3.95 % and 1320 % respectively. This is significantly higher than the deviations with case E (membrane properties of the Evonik membrane in COSYMA). Especially the CH_4 concentrations in the off-gas stream show a relatively high deviation and, in contrast to case E, the simulated concentration is well above the limit. This leads to the conclusion that the permeability data from case E describes the biogas upgrading plant in Reinach AG better than the permeability data from case M. Therefore, further considerations will only be done considering case E.
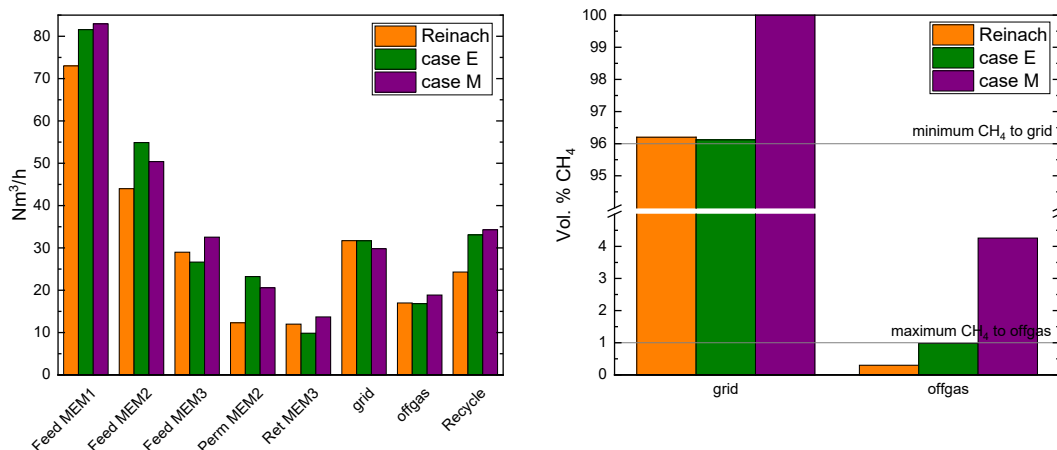

Figure 18: The Reinach AG plant compared with simulation results, operating point 1

The permeate from the second membrane shows the highest deviation (~89 %). The basis for this lies in the insufficient separation of CH_4 and CO_2 in the first membrane. The simulated retentate of MEM 1 (= feed MEM 2) already differs from the report data with almost 25 %, but because the retentate of MEM 2 (= grid stream) is nearly the same in both cases, the surplus volume flow is found in the permeate of MEM 2, which then leads to a bigger recycle and a bigger feed of MEM 1. A possible explanation are the different stages of development of the membrane modules used. Case E is based on experimental data from the membrane module in COSYMA, which was produced in 2012, whereas the modules in Reinach AG are from the same supplier but of a newer type (from 2015). For case E, it is suggested that in the first separation step, the membrane performance is not good enough to separate the CO_2 sufficiently. In the second separation step, with lesser CO_2 still present, the performance is sufficient, resulting in good results for the grid stream. Even though the newer membrane type was considered with a factor 1.5 bigger membrane area, the aforementioned considerations are still valid because, as mentioned in 4.1, the membrane modules in Reinach AG are characterized by different gas permeabilities in each separation step.

All in all, the validation of the rate-based membrane model is considered successful. Except for the permeate of MEM 2, the deviation between report data and simulation data is never more than 37 % for the volume flows. The considerations above suggest even better results with adjusted permeability data for the respective membrane modules. Sellaro et al. [28] strengthen that by saying that a multistage membrane system with highly permeable but less selective membranes in the first stages and highly selective but less permeable membranes in the successive stages is a good solution for achieving a high concentration of the desired species in the retentate and the permeate respectively.

5.2   Reference case for 0 % methanation

The necessary number of membrane modules for a fictitious industrial-scale (200 Nm^3/h) two-stage membrane process for biogas upgrading is summarized in Table 10. Even though 190 modules sound a lot at first, it has to be considered that this amount is referring to a membrane area of approximately 16.28 m^2 from the module in COSYMA. Using modules with a larger diameter and improved permeability (e.g. the ones from Reinach AG), this amount can be reduced to 32 modules (factor 6) or less.

The results show a big deviation between the cases E and M. This can be traced back to the significant differences between the two cases. While case M is a value from literature ([21]), studied under laboratory conditions for Matrimid® 5218, case E was acquired during field tests with an Evonik membrane of presumably similar material (no information about the exact material of the module in COSYMA is available). For both cases, the number of modules necessary for the first separation step is higher than the one for the second separation step. With a biogas composition in the membrane feed of approximately 72 % CO_2 and 28 % CH_4 (case E) and 62 % CO_2 and 38 % CH_4 (case M) respectively, this is not surprising, because the upgrading in the first step is very effortful, considering that the CH_4 concentration in the

retentate has to be over 96 %. In the second upgrading step, the feed composition is approximately 88 % CO_2 and 12 % CH_4 (Case E) and 86 % CO_2 and 14 % CH_4 (Case M) respectively, with a CH_4 concentration of less than 1 % required in the permeate.

Table 10: Necessary number of membrane modules for 200 Nm³/h biogas upgrading at 15 bar

membrane	-	1	2
case	E	190	33
	M	45	15

5.3 Reference case for 100 % methanation (full Power-to-Gas)

Using the number of membrane modules for the first membrane from the biogas upgrading scenario (Table 10), the full PtG setup with two compressors could meet the grid injection requirements in all four cases (see Figure 19). The abbreviations identify the different cases, where l and h respectively stand for lower or higher gas velocity and the second letter for the permeability case. When determining the permeability data for case E (Evonik membrane in COSYMA), the permeability of water was not established. Therefore, the results for both cases were standardized to dry mole fractions. This is a plausible assumption because in reality there would either be a drying step before the membrane unit or the water would mostly permeate through.
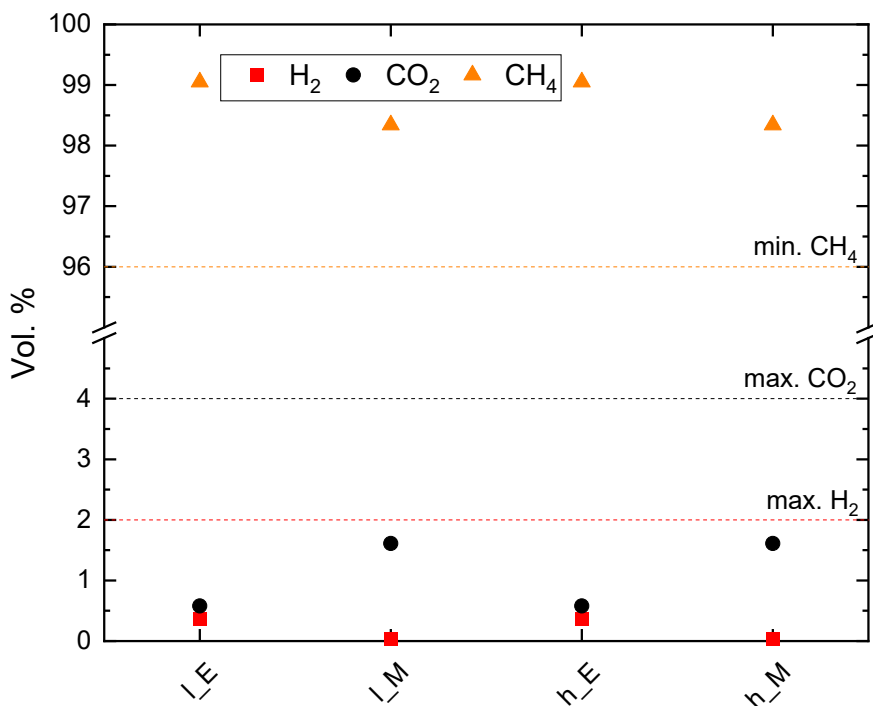

Figure 19: Grid compliance, f-PtG; l, h: lower/higher gas velocity; E, M: membrane properties

The reactor parameters of the four f-PtG cases are summarized in Table 11. The diameter and height refer to the catalyst bed. Here the effect of different gas velocities is clearly visible. A higher gas velocity results in a thinner but higher reactor with a diameter to height ratio below 1. The resulting differences in reactor dimensions are more significant between the gas velocities than the ones between the two different upgrading membrane types. As the gas velocity does not influence the conversion rate (CO_2 conversion for both gas velocities is nearly identical), the necessary catalyst mass as well as the produced reaction heat is nearly the same for both cases.

Table 11: Reactor parameters at 15 bara system and 2 bara permeate pressure, f-PtG

gas velocity	-	lower		higher	
case	-	E	M	E	M
reactor diameter	m	0.79	0.75	0.68	0.65
expanded bed height	m	0.53	0.56	0.70	0.74
CO_2 conversion	%	94.8	95.2	94.8	95.2
catalyst	kg	88.5	85.5	88.5	85.5
reaction heat	kW	176	171	176	171
main compressor	kW	37.4	33.2	37.4	33.2
second compressor	kW	9.61	7.51	9.61	7.51

5.3.1 Full Power-to-Gas with one compressor

In the case of f-PtG-1, the number of membrane modules had to be adjusted. After a first adaption with a reactor and permeate pressure of 6 bara, some problems occurred with the numerical stability of the membrane model for case E. Therefore, the reactor and permeate pressure were reduced to 4 bara with the results shown in Table 12. For comparability reasons, this was done for both cases even though case M could be simulated with a permeate and reactor pressure of 6 bara. Compared to two compressors and a system pressure of 15 bara, the number of membrane modules for both cases need to be more than 1.7 times as high to meet the grid injection requirements. With a higher system pressure, the number of necessary membrane modules is reduced. This is due to an increased pressure difference between the high- and low-pressure side of the membrane, which enhances its performance. At a system pressure of 20 bara and a permeate pressure of 4 bara, the grid injection requirements can be met with the same number of necessary membrane modules for MEM 1 like the biogas upgrading scenario at 15 bara (Table 10) with both membrane properties. This suggests that the one compressor option with a system pressure of 20 bara and a permeate pressure of 4 bara could be operated at the biogas upgrading plant from 5.2 using the same membrane unit.

Table 12: Necessary number of membrane modules, f-PtG-1

permeate pressure	bara	4					
system pressure	bara	15		18		20	
case	-	E	M	E	M	E	M
membrane modules	-	330	80	220	50	190	45

The reactor parameters of the twelve f-PtG-1 cases are summarized in Table 13 and were calculated with the respective number of membrane modules from Table 12. Compared to the f-PtG option (Table 11), the diameter to height ratio is bigger for the f-PtG-1 option at 15 bara. Even with the higher gas velocity, the ratio is above 1 in all cases. This can be led back to the lower pressure in the reactor. The reduced CO_2 conversion compared to the two compressor options results from a limited mass transfer, which is also caused by the lower pressure in the reactor.

To compare the f-PtG with the f-PtG-1 option, a preliminary cost comparison was made, with the results shown in Table 14. For f-PtG-1, only the case with a system pressure of 20 bara was considered, due to the results in Table 12. The calculations were performed according to the formulas, correlations and prices from [29]. The formulas and input parameters can be found in the appendix (Table 21). The compressor costs refer to centrifugal compressors and as the number of membrane modules is the same for both options, the membrane costs were not considered. The cost for the process vessel depends, among other things, on the reactor diameter. The referenced book considers the following diameters: 0.3 m, 0.5 m, 1 m, 1.5 m, 2 m, 2.5 m, 3 m and 4 m; therefore the actual diameter was rounded up to the next available one. The obtained reactor height was multiplied by a factor of 1.5 to assure sufficient heat removal and to prevent a possible deactivation of the catalyst by sulphur. At the end of the thesis, an error in the reactor model was found. For the calculation of the initial gas velocity and the heat exchanger surface, a wrong temperature was assumed, which influences the reactor dimensions. With the correct temperature, the diameter would tend to be smaller. This does not change the chemistry of the reaction, though, because the reaction takes place in thermodynamic equilibrium which was also included in the old model. Therefore, not all the cases were recalculated with the corrected reactor model. It would have been too time-consuming and would not have changed the key messages of the thesis. Only for the cost comparison, the dimensions were recalculated (see Table 21) to be able to make a correct statement. The referenced book indicates costs from 2004, a price adjustment was not considered necessary, since this is only a relative cost comparison and not a calculation of the absolute cost. With the considered prices and formulas for the total acquisition cost of the compressors, the process vessel and the internal heat exchanger, the one-compressor option is the cheaper choice for both upgrading membrane types. The two-compressor option is 12 % more expensive for case E and 11 % for case M respectively, related to the total cost of the two-compressor option. This is because the one compressor option does not need a

significantly higher overall compressor capacity, and requires a smaller reactor height as well as a lower reactor pressure. When comparing the two membrane types, case M seems to be the cheaper choice for f-PtG as well as f-PtG-1, but as no information about the cost of the two different membrane types is available, it is not clear if this statement is correct. This, however, does not change the fact that if a new plant is built, the capital costs for f-PtG-1 are cheaper than for f-PtG with the considered parameters.

Table 13: Reactor parameters at different system pressures and 4 bara permeate pressure, f-PtG-1

gas velocity	-	lower						higher					
system pressure	bara	15		18		20		15		18		20	
case	-	E	M	E	M	E	M	E	M	E	M	E	M
reactor diameter	m	1.01	0.94	0.98	0.92	0.97	0.92	0.87	0.81	0.85	0.80	0.84	0.79
expanded bed height	m	0.33	0.35	0.34	0.36	0.35	0.37	0.43	0.47	0.45	0.48	0.46	0.49
CO_2 conversion	%	93.2	93.9	93.6	94.2	93.8	94.3	93.2	93.9	93.6	94.2	93.8	94.3
catalyst	kg	90.3	84.5	88.9	83.6	88.3	83.6	90.4	84.5	88.9	83.6	88.3	83.6
reaction heat	kW	177	167	175	165	174	166	177	167	175	165	174	166
main compressor	kW	43.7	36.3	44.3	38.4	45.2	40.0	43.7	36.3	44.3	38.4	45.2	40.0

Table 14: Preliminary cost comparison of f-PtG and f-PtG-1 at the lower gas velocity

	two compressors				one compressor			
system pressure	15 bara				20 bara			
permeate pressure MEM 1	2 bara				4 bara			
reactor pressure	6 bara				4 bara			
	capacity [kW]		total cost [$]		capacity [kW]		total cost [$]	
case	E	M	E	M	E	M	E	M
main compressor	37.3	32.8	210,505	188,337	45.9	41.0	252,796	228,712
second compressor	9.55	7.27	73,368	62,054	-	-	-	-
process vessel			46,277	47,511			36,876	37,806
internal heat exchanger			594	583			590	581
acquisition cost [$]			**330,744**	**298,485**			**290,262**	**267,098**

Using the number of membrane modules from Table 12, the grid stream concentrations for f-PtG-1 were calculated and are displayed in Figure 20. The abbreviations identify the different cases, where l and h respectively stand for lower or higher gas velocity, the second letter for the different upgrading membrane types and the number for the system pressure. The results for both permeability data were standardized to dry mole fractions. With a permeate and reactor pressure of 4 bara, the grid injection requirements could be met in all scenarios. Figure 19 shows that the CH_4 concentration in the grid stream for f-PtG with the chosen number of membrane modules is very high (over 99 % for case E, over 98 % for case M), suggesting that with a decrease in membrane modules, the requirements can still be met. The same applies to f-PtG-1, with the CH_4 concentration in the grid stream being over 98 % for case E and over 97 % for case M. With the same number of membrane modules, the CH_4 concentration is higher for f-PtG compared to f-PtG-1. This suggests that in case the same CH_4 concentration is targeted, f-PtG will need a smaller number of membrane modules. For a more accurate cost comparison, these considerations have to be taken into account. Since the focus of this thesis is on the investigation of partial load behaviour in a fluidized-bed methanation reactor and a possible operation of three different process models in one plant, the cost analysis will not be pursued further.
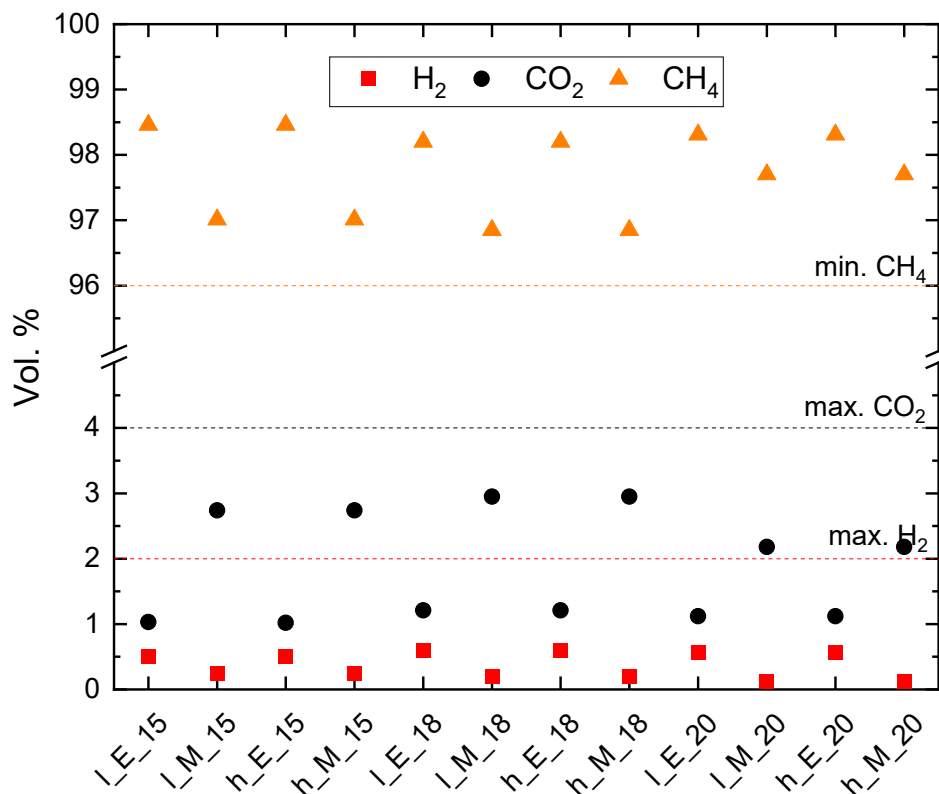

Figure 20: Grid compliance, f-PtG-1; l, h: lower/higher gas velocity; E, M: membrane properties; 15, 18, 20: system pressure

5.4   Full-load experiments with COSYMA

Figure 21 shows the grid compliance results for the full-load proof-of-concept experiments with COSYMA. The experiments were successful, as in most cases the grid injection requirements could be met, in the remaining cases the H_2 concentration slightly exceeded the limit of 2 %. Out of three different H_2 inputs, the one with an H_2 input of 49.5 Nl/min showed the most stable and replicable results and was thus defined as the maximum operable load. The 49.5 Nl/min were the basis for the calculation of the partial loads in 5.6. The results also showed that a plant operation with a recycle stream is feasible.

To meet the H_2 requirements was the biggest challenge during the full-load experiments with COSYMA. The manual operation required high alertness of the plant operators to act quickly in case of an H_2 or CO_2 accumulation in the system. Before the full-load experiments with recycle, a test run without a recycle stream was conducted. Higher H_2 inputs (up to 67 Nl/min) were feasible but they also resulted in H_2 concentrations above 2 % in the retentate stream with a permeate pressure of 1.2 bara. Nonetheless, these test runs showed that the fluidized-bed reactor in COSYMA is capable of a wider load range, with the membrane unit being the limiting factor. With an extendable modular set up of the membrane unit, the retentate could be processed to meet the grid injection requirements.
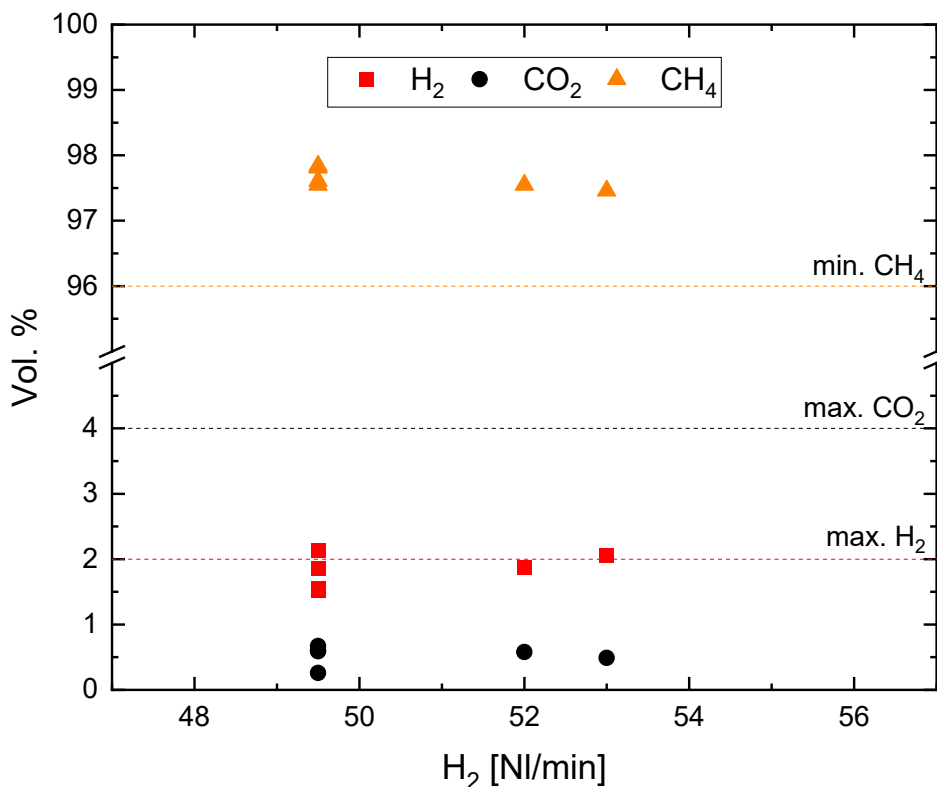

Figure 21: Full-load experiments with COSYMA, grid compliance

5.5 Partial-load Power-to-Gas

To simulate that the pl-PtG scenarios take place in the same plant as the biogas upgrading and the f-PtG scnearios, the number of membrane modules from the 0 % methanation scenario (Table 10) and the reactor parameters from the 100 % methanation scenario (Table 11) were used to calculate the concentration in the grid stream. With the given number of membrane modules, there were numerical problems with the membrane model for a lot of case E cases. This was partly due to an excess number of membrane modules. With low partial loads, the volume flow per module was less than 5 Nl/min, but the experiments to determine case E were conducted with 40 Nl/min or more. It was determined that the current membrane model does not function correctly with little volume flows per module, due to the numerical stiffness of the separation problem. For this reason, the number of membrane modules was recalculated to meet the condition of 40 Nl/min per module. In practice, part of the modules would be shut off to increase the volume flow per module. For some cases, the simulation did still not work, now due to problems with the reactor model. It is assumed that the volume flow into the reactor was too little compared to the defined reactor dimensions. Therefore, the reactor pressure was reduced from 6 bara to 4 or even 2 bara where necessary to expand the gas and increase the volume flow, which one would also do in reality when the fluidization in the reactor is too low. With the adapted number of membrane modules and reactor pressure, the grid injection requirements could not always be met, because a lower reactor pressure decreases the CO_2 conversion rate. For this reason, the number of membrane modules was increased again to enhance the separation of CH_4 and CO_2. Just one case with the membrane material Matrimid (6_M_20) needed adaption. Supposedly also because the volume flow into the reactor was too little. Table 15 displays the nine cases in which adaptions were necessary. The other eleven cases could successfully be simulated with the original parameters (see Table 10 and Table 11). Since the number of membrane modules is decreased compared to the 0 % methanation scenario and the reactor dimensions stay the same as in the full PtG scenario, the suggested adaptions can easily be realized at the suggested industrial plant due to the modular setup of the membrane unit. With intelligent process management and monitoring, the lifespan of the membrane modules can consequently be increased.

Table 15: Cases with adapted parameters, pl-PtG

gas velocity	-	l	h	l	h	l	h	l	l	h
case	-	E	E	E	E	E	E	E	M	E
partial load	%	50	50	40	40	30	30	20	20	20
reactor pressure	bara	4	6	4	4	2	4	2	4	2
membrane modules	-	80	78	64	64	50	48	33	45	33

The reaction parameters for all pl-PtG cases are displayed in Table 16. For the cases l_E_30, l_E_20 and h_E_20, the reactor pressure is the same as the permeate pressure (see Table 15), therefore the second compressor is not needed. The reaction heat and compressor

capacities increase with higher partial loads. This is not surprising since a higher partial load signifies a higher feed stream and thus a higher CO_2 volume flow. The higher feed stream results in higher compressor capacities and the higher CO_2 volume flow increases the strongly exothermic methanation reaction and thus the reaction heat. With a few exceptions, the CO_2 conversion rate also increases with a higher partial load. The exceptions can be explained with the adaptions shown in Table 15. The cases I_E_30 and I_M_20 operate with lower reactor pressures compared to h_E_30 and h_M_20 respectively, which results in a shift of the chemical equilibrium to the reactants' side and thus a lower CO_2 conversion rate. Case h_E_50 operates with the same pressure as cases I_E_75 and h_E_75, but with a significantly lower number of membrane modules and thus a different composition in the permeate and consequently the reactor feed stream. While the reactor feed for I_E_75 and h_E_75 consists of approximately 16 % CO_2 and 22 % CH_4, the reactor feed for h_E_50 consists of approximately 17 % CO_2 and 15 % CH_4, which is presumably the reason for the better CO_2 conversion rate.

Table 16: Reaction parameters, pl-PtG

	CO_2 conversion	reaction heat	main compressor	second compressor		CO_2 conversion	reaction heat	main compressor	second compressor
	%	kW	kW	kW		%	kW	kW	kW
I_E_75	94	134	30.4	8.5	I_M_75	95	132	26.4	6.4
h_E_75	94	134	30.4	8.5	h_M_75	95	132	26.4	6.5
I_E_50*	94	87	18.2	2.7	I_M_50	95	89	19.5	5.3
h_E_50*	95	87	17.8	4.3	h_M_50	95	89	19.5	5.3
I_E_40*	94	70	14.5	2.2	I_M_40	94	72	16.7	4.8
h_E_40*	94	70	14.5	2.2	h_M_40	94	72	16.7	4.8
I_E_30*	92	53	11.4	0	I_M_30	94	54	13.9	4.3
h_E_30*	94	52	10.9	1.6	h_M_30	94	54	13.9	4.3
I_E_20*	92	35	7.6	0	I_M_20*	92	36	11.2	2.4
h_E_20*	92	35	7.6	0	h_M_20	93	36	11.1	3.8

*adapted cases, for adaptions see Table 15

Figure 22 shows the composition of the grid stream for all pl-PtG cases, where the adapted cases are marked. The abbreviations identify the different cases, where l and h respectively stand for lower or higher gas velocity, the second letter indicates the different upgrading membrane types and the number stands for the partial load. The results for both membrane properties were standardized to dry mole fractions. Concerning the adapted cases, it shows that the suggested measures (reducing the reactor pressure and decreasing the number of membrane modules) are working. This finding is also helpful for the operation of industrial plants. Case M shows very high concentrations of CH_4 in the grid stream, which increase with

a decreasing partial load, suggesting that a decrease in the number of membrane modules is possible. The same applies to case E. With a decrease in the number of necessary membrane modules for the pl-PtG scenarios, the lifespan of the modules can be extended, which decreases the operating costs. Within the limits for the membrane unit from the 0 % methanation scenario and the limits for the reactor dimensions from the f-PtG scenario, a partial load of 20 % is feasible with the chosen pl-PtG configuration for both membrane properties.
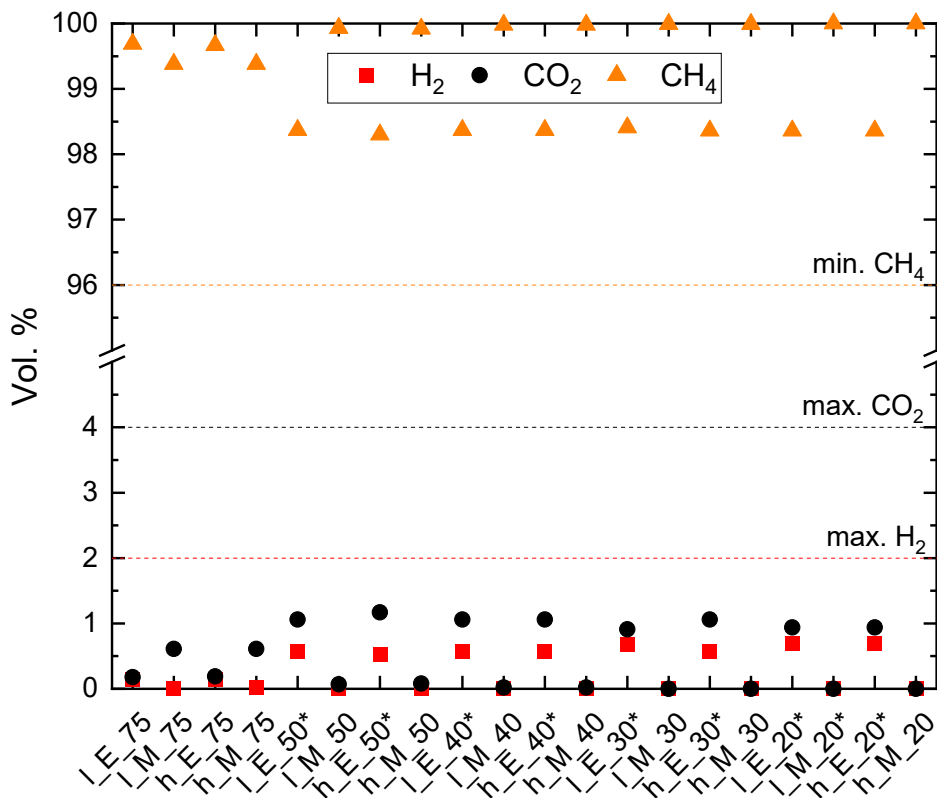
Figure 22: Grid compliance, pl-PtG; l, h: lower/higher gas velocity; E, M: membrane properties; 75, 50, 40, 30, 20: partial load [%]; *adapted cases, for adaptions see Table 15

5.5.1   Partial load Power-to-Gas with one compressor

Using the number of membrane modules and the reactor dimensions from the f-PtG-1 scenario (Table 12 and Table 13), the grid stream concentrations for the pl-PtG-1 cases were calculated. For all cases with the Evonik membrane type, the same problems as with the pl-PtG cases occurred. Therefore, the same adaptions – setting the volume flow per module to 40 Nl/min, possibly reducing the reactor pressure and increasing the number of membrane modules again – were made. The necessary adaptions are displayed in Table 17. At a partial load of 50 %, the simulation shows that a higher gas velocity makes it possible to keep the reactor pressure at a higher level and thus enhance the reaction kinetics. For all cases with the Evonik

membrane properties and a partial load of 20 %, the simulation did not work, even though the suggested adaptions were made. The volume flow into the reactor is very little compared to the Matrimid cases at the same partial load. The assumption is that the reactor model cannot handle too little input flows. Except for two, all the cases with the Matrimid membrane type could successfully be simulated with the original parameters (see Table 12 and Table 13). For I_M_20 at a system pressure of 18 and 20 bara, the reactor pressure had to be reduced from 4 to 2 bara for the simulation to converge. An adaption of the volume flow per module was not made, thus the number of membrane modules stayed the same. As with pl-PtG, the number of membrane modules for pl-PtG-1 is decreased compared to the 0 % methanation scenario and the reactor dimensions stay the same as in the full PtG scenario, therefore the suggested adaptions can easily be realized at the suggested industrial plant due to the modular setup of the membrane unit.

Table 17: Cases with adapted parameters, pl-PtG-1

system pressure		15							
gas velocity	-	l	h	l	h	l	h	l	h
case	-	E	E	E	E	E	E	E	E
partial load	%	75	75	50	50	40	40	30	30
reactor pressure	bara	4	4	2	4	2	2	2	2
membrane modules	-	190	190	84	120	67	67	50	50
system pressure		18							
gas velocity	-	l	h	l	h	l	h	l	h
case	-	E	E	E	E	E	E	E	E
partial load	%	75	75	50	50	40	40	30	30
reactor pressure	bara	4	4	2	4	2	2	2	2
membrane modules	-	130	130	87	90	70	70	52	52
system pressure		20							
gas velocity	-	l	h	l	h	l	h	l	h
case	-	E	E	E	E	E	E	E	E
partial load	%	75	75	50	50	40	40	30	30
reactor pressure	bara	4	4	2	4	2	2	2	2
membrane modules	-	123	123	89	82	71	71	53	53

The reaction parameters for all pl-PtG-1 cases are displayed in Table 18. The observations are the same as with the pl-PtG cases. With a lower reactor pressure, the CO_2 conversion rate decreases (see Table 18 l_E_50 compared to h_E_50 for all system pressures). The influence of a lower reactor pressure on the CO_2 conversion rate is also visible in the cases with Matrimid membrane properties. The two adapted cases (l_M_20 at 18 and 20 bara system pressure) have CO_2 conversions of 88 % compared to 90 % at a system pressure of 15 bara where no adaptions were necessary.

Table 18: Reaction parameters, pl-PtG-1

system pressure		CO$_2$ conversion	reaction heat	main compressor		CO$_2$ conversion	reaction heat	main compressor
bara		%	kW	kW		%	kW	kW
15	l_E_75*	94	130	29.8	l_M_75	94	131	29.5
	h_E_75*	94	130	29.8	h_M_75	94	131	29.5
	l_E_50*	92	88	19.1	l_M_50	93	90	22.7
	h_E_50*	94	86	19.5	h_M_50	93	90	22.6
	l_E_40*	92	70	15.3	l_M_40	92	72	19.8
	h_E_40*	92	70	15.3	h_M_40	92	72	19.8
	l_E_30*	92	53	11.4	l_M_30	92	54	16.9
	h_E_30*	92	53	11.4	h_M_30	92	54	16.9
	l_E_20	-	-	-	l_M_20	90	36	14.0
	h_E_20	-	-	-	h_M_20	90	36	14.0
18	l_E_75*	94	128	31.0	l_M_75	94	130	30.8
	h_E_75*	94	128	31.0	h_M_75	94	130	30.8
	l_E_50*	92	89	22.1	l_M_50	93	89	23.3
	h_E_50*	94	86	20.9	h_M_50	93	89	23.3
	l_E_40*	92	71	17.7	l_M_40	93	72	20.1
	h_E_40*	92	71	17.7	h_M_40	93	72	20.1
	l_E_30*	92	53	13.2	l_M_30	92	54	16.9
	h_E_30*	92	53	13.2	h_M_30	92	54	16.9
	l_E_20	-	-	-	l_M_20*	88	36	15.3
	h_E_20	-	-	-	h_M_20	91	36	13.7
20	l_E_75*	94	130	33.1	l_M_75	94	131	33.0
	h_E_75*	94	130	33.1	h_M_75	94	131	33.0
	l_E_50*	92	89	24.0	l_M_50	93	89	24.9
	h_E_50*	94	86	22.1	h_M_50	93	89	24.9
	l_E_40*	92	71	19.2	l_M_40	93	72	21.5
	h_E_40*	92	71	19.2	h_M_40	93	72	21.5
	l_E_30*	92	54	14.3	l_M_30	92	54	18.1
	h_E_30*	92	54	14.3	h_M_30	92	54	18.1
	l_E_20	-	-	-	l_M_20*	88	36	16.3
	h_E_20	-	-	-	h_M_20	91	36	14.7

*adapted cases, for adaptions see Table 17

Figure 23 shows the composition of the grid stream for the pl-PtG-1 cases at the three different system pressures. The adapted cases are marked. The abbreviations identify the different cases, where l and h respectively stand for lower or higher gas velocity, the second letter indicates the different upgrading membrane types and the number stands for the partial load. The results for both membrane properties were standardized to dry mole fractions. At lower partial loads, case M shows very high concentrations of CH_4 in the grid stream, suggesting that a decrease in the number of membrane modules is possible, the same applies to case E. For the 75 % and partly the 50 % partial-load cases, the CH_4 concentration is closer to the limit of 96 %, an increase in membrane modules can change the concentration ratio to safely meet the grid injection requirements. Within the limits for the membrane unit from the 0 % methanation scenario and the limits for the reactor dimensions from the f-PtG-1 scenario, a partial load of 20 % is feasible with the chosen pl-PtG-1 configuration and the Matrimid membrane properties. For the Evonik membrane properties in the present configuration, the minimum partial load is at 30 %.
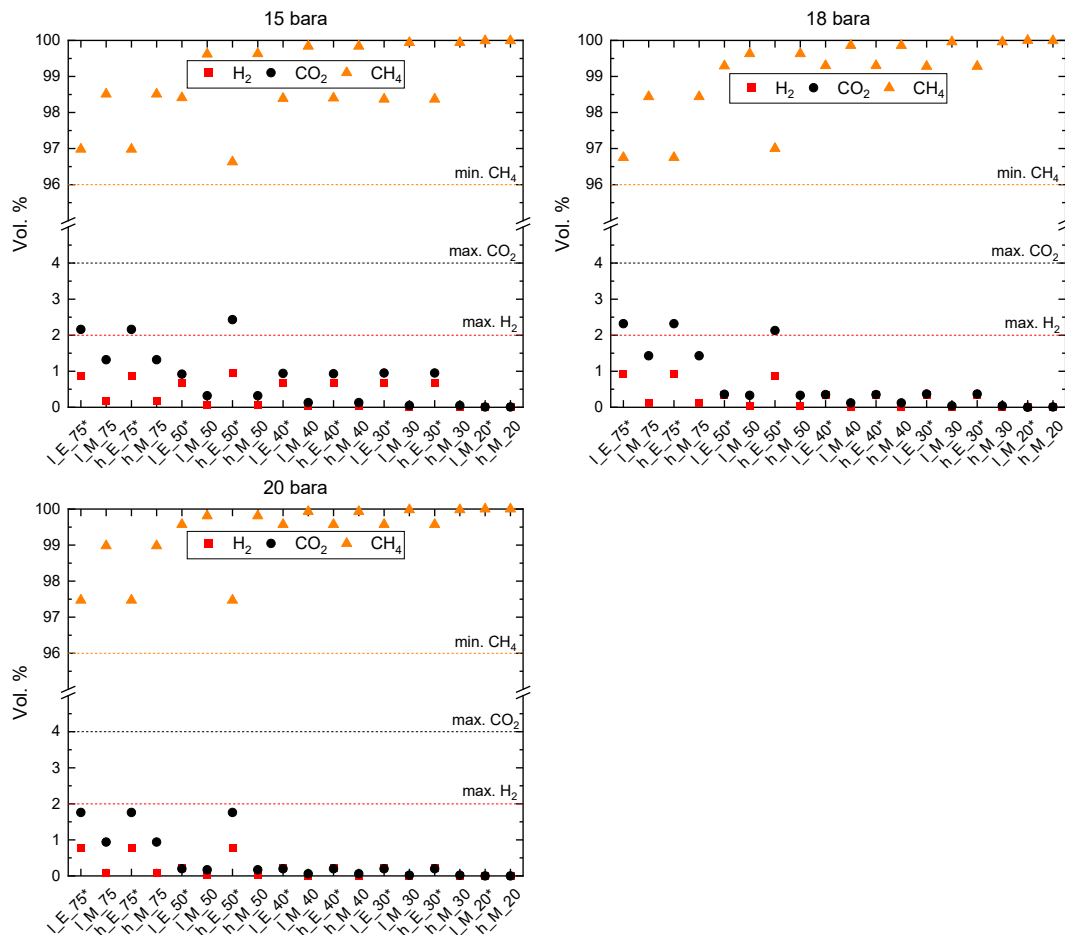
Figure 23: Grid compliance, pl-PtG-1; l, h: lower/higher gas velocity; E, M: membrane properties; 75, 50, 40, 30, 20: partial load [%]; *adapted cases, for adaptions see Table 17

5.6   Partial-load experiments with COSYMA

Figure 24 shows the grid compliance results for the partial-load proof-of-concept experiments with COSYMA. The experiments were successful, as in most cases the grid injection requirements could be met. In cases where the requirements were not met at the first try, follow-up experiments with the same input parameters were conducted to show that compliance is possible with an adjusted plant handling. The minimum partial load for COSYMA with a recycle stream was determined at around 40 %. But also other partial loads (~ 55 %, ~ 63 %, ~ 77 %) could successfully be replicated and stand-alone experiments for ~ 80 and ~ 87 % were conducted as well. This suggests that a continuous dynamic operation of a fluidized-bed reactor in the configuration of COSYMA with a recycle stream is possible for loads between 40 and 100 %.

Also for the partial-load experiments, meeting the H_2 requirements was the biggest challenge. And as with the full-load experiments, there were test runs for the partial-load experiments without recycle conducted beforehand. Compared to the full-load test runs without recycle, a partial load of 20 % was feasible in the reactor. The membrane unit and the compressor were the limiting factors, with the H_2 concentration in the retentate being at around 10 %. Nonetheless, these test runs showed again that the fluidized-bed reactor in COSYMA is capable of a wider load range.
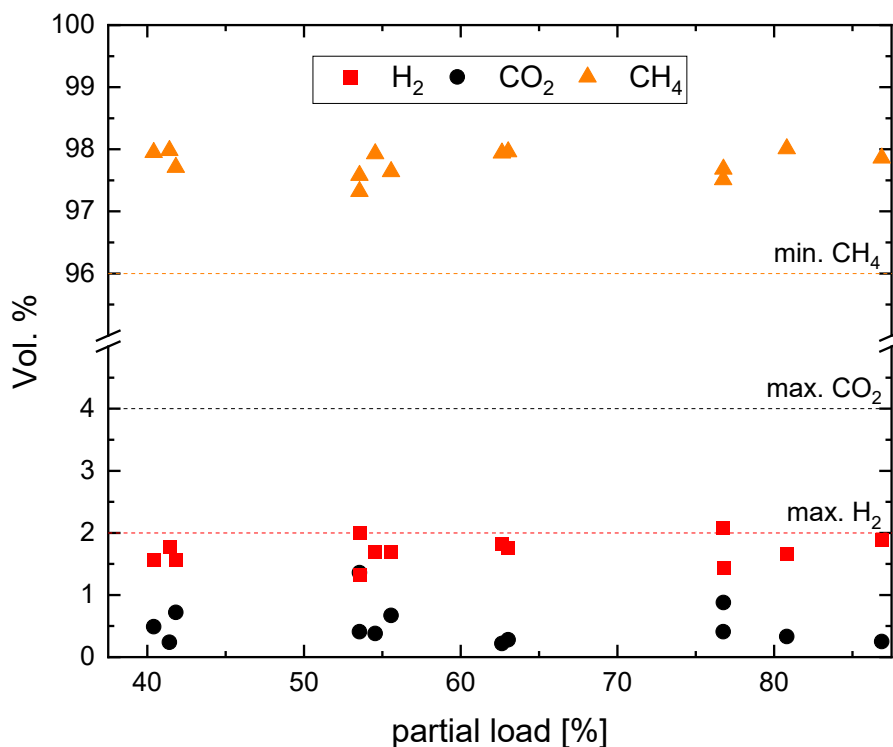
Figure 24: Partial-load experiments with COSYMA, grid compliance

6   Summary and conclusion

The worldwide trend of increasing the variable renewable energy production while shutting down conventional energy plants like nuclear and coal power plants demands new solutions for the stability of the power grid and a continuous energy supply. In terms of energy storage, the Power-to-Gas concept is a promising approach. With the surplus energy from volatile energy production like solar and wind, H_2 is produced via electrolysis. In a further but optional process step, the produced H_2 together with a CO_2 source, e.g. from a biogas plant, is converted to methane (CH_4). Producing CH_4 instead of H_2 has the advantage of an existing storage and distribution grid. Furthermore, CH_4 can be used in various applications and has a high volumetric energy storage density. The gas catalytic methanation reaction is strongly exothermic and requires good heat management to not damage the catalyst or the reactor. To tackle this challenge, various reactor concepts were developed. Here, a fluidized-bed reactor is used. It has the advantage of an approximately isothermal temperature profile and reduced mass transfer limitations, due to the movement of particles. This facilitates the control of the operation and allows for using one single reactor with a rather simplified design. To respond to the transient energy and H_2 production, a flexible operation of the reactor is necessary. The feasibility of various partial loads and the limits are investigated in this thesis.

Prior to this thesis, different variants for an innovative approach for biogas upgrading plants were developed, the difference being in the arrangement of the methanation reactor and the membrane unit in relation to each other. The idea is a year-round operation in different utilization stages. In winter, with a higher energy demand and lower surplus energy from volatile production, it is purely a biogas upgrading plant using a membrane unit without the methanation step (0 % methanation). In summer, with high levels of surplus energy from volatile production, the plant would operate in full Power-to-Gas mode, producing methane at full-load and steady-state conditions (100 % methanation). In the intermediate seasons spring and autumn, the plant would operate in the mode of partial-load Power-to-Gas. To be able to efficiently use as much surplus energy as possible and to make the process chain less sensitive to high electricity prices, the methanation reactor is required to have a wide load range with partial loads as low as possible. Determining the parameters which have the biggest effect to reach lower partial loads and how to configure them is one of the key messages of this thesis.

The present thesis investigates the partial-load behaviour of one variant for a biogas upgrading plant with a membrane unit and a following fluidized-bed methanation reactor in a MATLAB-based simulation toolbox. The development of the membrane and reactor model respectively was not part of the remit but was conducted at PSI prior to the start of this thesis. Different membrane properties, gas velocities, system pressures and numbers of available compressors were tested to determine the feasibility limits. A preliminary cost comparison between the two and one compressor option was conducted as well. Besides the various simulation scenarios, proof-of-concept experiments were conducted on a pilot plant. The process configuration in

the pilot plant is not the same as in the simulations, but the experiments were intended to demonstrate the feasibility of partial load in a fluidized-bed methanation reactor with a recycle of the permeate stream.

The 0 % methanation case was intended to determine the dimensions of the membrane unit for the whole plant. The investigations proved that this assumption was correct. For the full- and partial-load PtG cases with two compressors, the number of membrane modules for MEM 1 obtained from the 0 % methanation case was sufficient to meet the grid injection requirements. Especially for the partial-load cases, even a smaller number of modules would be sufficient, which is no problem in the process management due to the modular setup of the membrane unit. For the full- and partial-load cases with one compressor, the permeate pressure needed to be equal to the value of the reactor pressure. Therefore, the pressure difference in the membrane unit decreased and consequently the number of membrane modules increased. After increasing the system pressure to 20 instead of 15 bara and decreasing the reactor pressure to 4 instead of 6 bara, the same number of membrane modules as in the 0 % methanation case was sufficient to meet the grid injection requirements. When building a new plant, the one compressor option is the cheaper choice according to a preliminary cost comparison. However, the two compressor option is more stable because the reactor and permeate pressure can be set independently, and can also be implemented when expanding an already existing biogas upgrading plant.

With the 100 % methanation case, it was intended to determine the reactor dimensions for the whole plant. The investigations showed that partial loads down to 20 % are possible with the obtained reactor dimensions. The problem with too little partial loads can be an insufficient turbulence of the catalyst particles because the necessary force for the fluidization applied by the volume flow is too little. It was shown that a decrease in the reactor pressure is helpful to overcome this challenge. Even though the CO_2 conversion rate is decreased in doing so, the grid injection requirements can still be met with an aligned number of membrane modules.

The proof-of-concept experiments showed promising results for the application of a BFB reactor in a flexible PtG system. With a recycle of the permeate stream, the minimum partial load was at around 40 %. Test runs without the recycle showed that the reactor is capable of partial loads down to 20 %. For this to be feasible with recycle, the compressor and the membrane unit need to be adjusted. While the compressor needs to be able to also process very little volume flows (the minimum of the current compressor is at ~ 35 % capacity), the membrane unit needs to be improved with additional modules.

This thesis shows that the presented innovative concept for biogas upgrading plants is technically feasible. An industrial-scale 200 Nm^3/h plant can be operated in different utilization stages all the year round. Due to the modular setup of the membrane unit, it can either be used for the sole purpose of biogas upgrading or it can be converted to a Power-to-Gas plant with possible loads of 20 to 100 %. For the economic feasibility, a detailed cost analysis as well as a comparison with the second variant (see Figure 9) is necessary. To prove that the simulations

are valid, follow-up experiments with the corresponding process management are necessary as well.

7 Lists

7.1 List of publications

[1] World Energy Council, "World Energy Perspectives VARIABLE RENEWABLES SYSTEMS : HOW TO GET IT RIGHT," *World Energy Perspect. Renew. Intergration*, no. september 2016, p. 140, 2016.

[2] E. Giglio, R. Pirone, and S. Bensaid, "Dynamic Modelling of Methanation Reactors During Start-up and Regulation in Intermittent Power-to-Gas Applications," *Renew. Energy*, vol. 170, pp. 1040–1051, 2021, doi: 10.1016/j.renene.2021.01.153.

[3] M. Götz *et al.*, "Renewable Power-to-Gas: A technological and economic review," *Renew. Energy*, vol. 85, pp. 1371–1390, 2016, doi: 10.1016/j.renene.2015.07.066.

[4] F. Bauer, C. Hulteberg, T. Persson, and D. Tamm, "Biogas upgrading – Review of commercial technologies," 2013.

[5] Evonik, "Factsheet: Sepuran Green - Membrane Technology for Efficient Biogas Upgrading," 2018, [Online]. Available: http://www.sepuran.com/product/peek-industrial/downloads/sepuran-green-for-upgrading-biogas-en.pdf.

[6] L. W. McKeen, "Markets and Applications for Films, Containers, and Membranes," *Permeability Prop. Plast. Elastomers*, pp. 59–75, Jan. 2012, doi: 10.1016/B978-1-4377-3469-0.10004-9.

[7] A. Makaruk and M. Harasek, "Numerical algorithm for modelling multicomponent multipermeator systems," *J. Memb. Sci.*, vol. 344, no. 1–2, pp. 258–265, 2009, doi: 10.1016/j.memsci.2009.08.013.

[8] M. Lehner, R. Tichler, H. Steinmüller, and M. Koppe, *Power-to-Gas: Technology and Business Models*. Springer International Publishing, 2014.

[9] G. A. Mills and F. W. Steffgen, "Catalytic methanation," *Catal. Rev.*, vol. 8, no. 1, pp. 159–210, 1974, doi: 10.1080/01614947408071860.

[10] J. Kopyscinski, T. J. Schildhauer, and S. M. A. Biollaz, "Production of synthetic natural gas (SNG) from coal and dry biomass - A technology review from 1950 to 2009," *Fuel*, vol. 89, no. 8, pp. 1763–1783, 2010, doi: 10.1016/j.fuel.2010.01.027.

[11] S. Bajohr, M. Götz, F. Graf, and F. Ortloff, "Speicherung von regenerativ erzeugter elektrischer Energie in der Erdgasinfrastruktur," *GWF, Gas - Erdgas*, vol. 152, no. 4, pp. 200–209, 2011.

[12] J. Lefebvre, M. Götz, S. Bajohr, R. Reimert, and T. Kolb, "Improvement of three-phase methanation reactor performance for steady-state and transient operation," *Fuel Process. Technol.*, vol. 132, pp. 83–90, Apr. 2015, doi: 10.1016/J.FUPROC.2014.10.040.

[13] P. Biegger, F. Kirchbacher, A. R. Medved, M. Miltner, M. Lehner, and M. Harasek, "Development of Honeycomb Methanation Catalyst and Its Application in Power to Gas Systems," *Energies 2018, Vol. 11, Page 1679*, vol. 11, no. 7, p. 1679, Jun. 2018, doi: 10.3390/EN11071679.

[14] K. P. Brooks, J. Hu, H. Zhu, and R. J. Kee, "Methanation of carbon dioxide by hydrogen reduction using the Sabatier process in microchannel reactors," *Chem. Eng. Sci.*, vol. 62, no. 4, pp. 1161–1170, Feb. 2007, doi: 10.1016/j.ces.2006.11.020.

[15] S. Matthischke, S. Roensch, and R. Güttel, "Start-up Time and Load Range for the Methanation of Carbon Dioxide in a Fixed-Bed Recycle Reactor," *Ind. Eng. Chem. Res.*, vol. 57, no. 18, pp. 6391–6400, 2018, doi: 10.1021/acs.iecr.8b00755.

[16] E. Inkeri, T. Tynjälä, A. Laari, and T. Hyppänen, "Dynamic one-dimensional model for biological methanation in a stirred tank reactor," *Appl. Energy*, vol. 209, no. October 2017, pp. 95–107, 2018, doi: 10.1016/j.apenergy.2017.10.073.

[17] R. W. Baker, "Membrane Gas-Separation: Applications," *Membr. Oper. Innov. Sep. Transform.*, pp. 167–194, Jul. 2009, doi: 10.1002/9783527626779.CH8.

[18] A. Gantenbein, J. Witte, S. M. A. Biollaz, O. Kröcher, and T. J. Schildhauer, "Flexible application of biogas upgrading membranes for hydrogen recycle in power-to-methane processes," *Chem. Eng. Sci.*, vol. 229, p. 116012, 2021, doi: 10.1016/j.ces.2020.116012.

[19] J. Kopyscinski, T. J. Schildhauer, and S. M. A. Biollaz, "Methanation in a fluidized bed reactor with high initial CO partial pressure: Part II- Modeling and sensitivity study," *Chem. Eng. Sci.*, vol. 66, no. 8, pp. 1612–1621, 2011, doi: 10.1016/j.ces.2010.12.029.

[20] J. Witte, J. Settino, S. M. A. Biollaz, and T. J. Schildhauer, "Direct catalytic methanation of biogas – Part I: New insights into biomethane production using rate-based modelling and detailed process analysis," *Energy Convers. Manag.*, vol. 171, no. December 2017, pp. 750–768, 2018, doi: 10.1016/j.enconman.2018.05.056.

[21] Y. Zhang, I. H. Musselman, J. P. Ferraris, and K. J. Balkus, "Gas permeability properties of Matrimid® membranes containing the metal-organic framework Cu-BPY-HFS," *J. Memb. Sci.*, vol. 313, no. 1–2, pp. 170–181, 2008, doi: 10.1016/j.memsci.2008.01.005.

[22] A. S. Calbry-Muzyka *et al.*, "Deep removal of sulfur and trace organic compounds from biogas to protect a catalytic methanation reactor," *Chem. Eng. J.*, vol. 360, no. November 2018, pp. 577–590, 2019, doi: 10.1016/j.cej.2018.12.012.

[23] J. Witte, A. Calbry-Muzyka, T. Wieseler, P. Hottinger, S. M. A. Biollaz, and T. J. Schildhauer, "Demonstrating direct methanation of real biogas in a fluidised bed reactor," *Appl. Energy*, vol. 240, no. September 2018, pp. 359–371, 2019, doi: 10.1016/j.apenergy.2019.01.230.

[24] SVGW Schweizerischer Verein des Gas- und Wasserfaches, *G13 d Richtlinie für die Einspeisung von erneuerbaren Gasen | SVGW*. 2016.

[25] C. Müller and U. Oester, "Biogasaufbereitungsanlage - Aufbereitung von 40 Nm3/h Klärgas zu Reingas und Einspeisung ins 5 bar-Erdgasnetz," 2019.

[26] "Patended 3-stage membrane-based separation process - Evonik Industries." https://www.membrane-separation.com/en/upgrading-of-biogas-to-biomethane-with-sepuran-green/3-stage-patent (accessed Aug. 09, 2021).

[27] T. Kvist and N. Aryal, "Methane loss from commercially operating biogas upgrading plants," *Waste Manag.*, vol. 87, pp. 295–300, Mar. 2019, doi: 10.1016/J.WASMAN.2019.02.023.

[28]   M. Sellaro, A. Brunetti, E. Drioli, and G. Barbieri, "CO2-CH4 Membrane Separation," pp. 14–17, 2015.

[29]   G. D. Ulrich and P. T. Vasudevan, *Chemical engineering process design and economics: a practical guide.* Process Publishing, 2004.

7.2   List of abbreviations

°C	degree Celsius
atm	atmosphere
BFB	bubbling fluidized bed
BGP	biogas plant
CH_4	methane
CO_2	carbon dioxide
CSTR	continuously stirred tank reactor
ΔG_R	Gibbs free enthalpy
ΔH_R	enthalpy of reaction
E	membrane properties of Evonik membrane
e.g.	exempli gratia (for example)
etc.	et cetera
f-PtG	full Power-to-Gas with two compressors
f-PtG-1	full Power-to-Gas with one compressor
g	gaseous / grams
H_2	hydrogen
H_2O	water
HEX	heat exchanger
kg	kilograms
M	membrane properties of Matrimid
m	metres
MFC	mass flow control
mGC	micro gas chromatograph
NDIR	nondispersive infrared sensor
Nl, Nml	standard litres, standard millilitres
p_perm	permeate pressure
pl-PtG	partial-load Power-to-Gas with two compressors
pl-PtG-1	partial-load Power-to-Gas with one compressor
PSI	Paul Scherrer Instiut
PtG	Power-to-Gas
s	solid
SFPI	Swiss Farmer Power Inwil
SNG	synthetic or substitute natural gas
TCP	thermo-chemical processes
TRL	technology readiness level
Vol. %	percent by volume

7.3　List of tables

7.4   List of figures

Appendix

Table 19: Remaining reactor parameters for the simulation of an industrial scale PtG plant

T_react	T_r_feed	T_gasMix	d_HEX_tubes	bubble_corr	H$_2$/CO$_2$
°C	°C	°C	m	case	mol/mol
360	280	175	0.025	6	4.01
H$_2$O/CO$_2$	T_preCond	T_mid	T_cond	gas velocity	Case
mol/mol	°C	°C	°C	-	-
0	180	80	40	lower	E
					M
				higher	E
					M

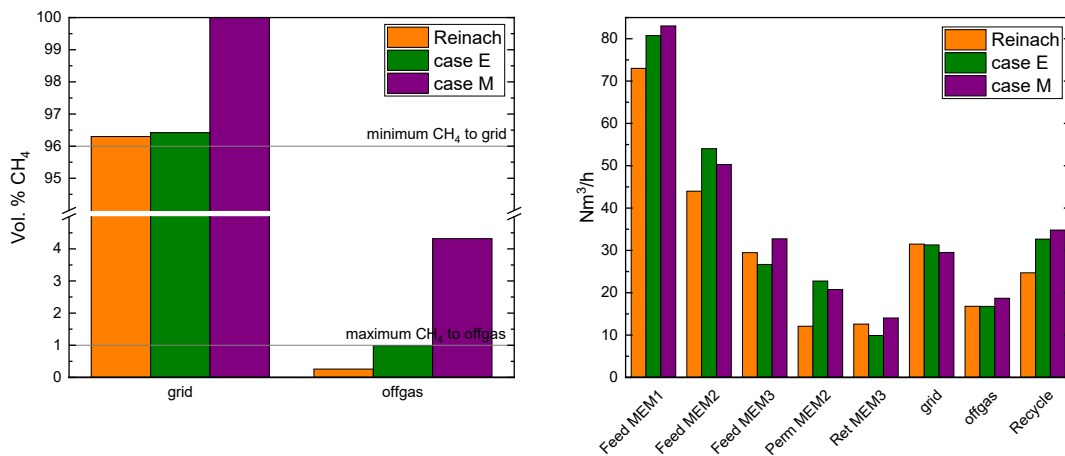Figure 25: The Reinach AG plant compared with simulation results, operating point 2

Formulas and factors for the calculations in Table 14:

$$compressor\ cost = CP_{comp} * FM_{comp}$$

$$CP_{comp} = 0.00001 * P_{comp}^3 - 0.1074 * P_{comp}^2 + 789.44 * P_{comp} + 4116.3$$

$$FM_{comp} = 6.3\ (stainless\ steel)$$

$$vessel\ cost = CP_{reac} * (1.7 * FP_{reac} * FM_{reac} + 2.6) + internal\ HEX\ cost$$

$$CP_{reac} = A * d_{reac}^2 + B * d_{reac} + C$$

$$FP_{reac} = -0.00007 * p_{reac}^2 + 0.0523 * p_{reac} + 0.95$$

$$FM_{reac} = 4\ (stainless\ steel)$$

$$internal\ HEX\ cost = CP_{HEX} * FM_{HEX}$$

$$CP_{HEX} = 1900 * \left(\frac{d_{HEX\_tubes}^2 * \pi * h_{reac} * N_{tubes}}{4}\right)^{0.5228}$$

$$FM_{HEX} = 1.7\ (stainless\ steel)$$

Table 20: Formula symbols

CP	equipment cost, bare	P_comp	capacity compressor
FM	material factor	FP	pressure factor
A, B, C	empirical parameters depending on the diameter		

Table 21: input parameters for the calculations in Table 14

	two compressors		one compressor	
system pressure	15 bara		20 bara	
permeate pressure	2 bara		4 bara	
reactor pressure	6 bara		4 bara	
case	E	M	E	M
reactor diameter [m]	0.73	0.69	0.86	0.83
reactor height*1.5 [m]	0.93	0.98	0.65	0.69
reactor pressure [bara]	6	6	4	4
N_tubes* [-]	237	217	335	306

*N_tubes = number of internal heat exchanger tubes